Quaternary Research 83 (2015) 187–203

Contents lists available at ScienceDirect

Quaternary Research

journal homepage: www.elsevier.com/locate/yqres

Directly dated MIS 3 lake-level record from Lake Manix, Mojave Desert, California, USA

Marith C. Reheis [a,*], David M. Miller [b], John P. McGeehin [c], Joanna R. Redwine [d], Charles G. Oviatt [e], Jordon Bright [f]

[a] U.S. Geological Survey, MS-980, Federal Center, Box 25046, Denver CO 80225, USA
[b] U.S. Geological Survey, MS-945, 345 Middlefield Rd., Menlo Park, CA 94025, USA
[c] U.S. Geological Survey, MS-926, National Center, 12201 Sunrise Valley Drive, Reston, VA 20192, USA
[d] U.S. Bureau of Reclamation, MS-86-25007, Federal Center, Box 25046, Denver, CO 80225, USA
[e] Department of Geology, Kansas State University, 108 Thompson Hall, Manhattan, KS 66506-3201, USA
[f] Department of Geosciences, University of Arizona, Tucson, AZ 85721, USA

ARTICLE INFO

Article history:
Received 11 June 2014
Available online 16 December 2014

Keywords:
Paleoclimate
Pluvial lake
Mojave Desert
Dansgaard–Oeschger cycles
Heinrich events

ABSTRACT

An outcrop-based lake-level curve, constrained by ~70 calibrated ^{14}C ages on *Anodonta* shells, indicates at least 8 highstands between 45 and 25 cal ka BP within 10 m of the 543-m upper threshold of Lake Manix in the Mojave Desert of southern California. Correlations of Manix highstands with ice, marine, and speleothem records suggest that at least the youngest three highstands coincide with Dansgaard–Oeschger (D–O) stadials and Heinrich events 3 and 4. The lake-level record is consistent with results from speleothem studies in the Southwest that indicate cool wet conditions during D–O stadials. Notably, highstands between 43 and 25 ka apparently occurred at times of generally low levels of pluvial lakes farther north as interpreted from core-based proxies. Mojave lakes may have been supported by tropical moisture sources during oxygen-isotope stage 3, perhaps controlled by southerly deflection of Pacific storm tracks due to weakening of the sea-surface temperature gradient in response to North Atlantic climate perturbations.

Introduction

The southwestern United States responds sensitively to climate change through variations in runoff (Enzel and Wells, 1997), pluvial lake size (e.g., Hostetler and Benson, 1990; Menking et al., 2004), and depth to groundwater (e.g., Quade, 1986; Quade et al., 1995; Pigati et al., 2011). Modern precipitation patterns vary due to fluctuating influences of the 3–7-yr cycle of El Niño-Southern Oscillation (ENSO), the Pacific Decadal Oscillation (PDO), the North American monsoon in part of the region (Hereford et al., 2006), and occasional intense atmospheric-river storms (e.g., Dettinger et al., 2011; Rutz and Steenburgh, 2012). Holocene lakes in this area are suggested to result from prolonged decadal periods of greatly increased rainfall (Enzel et al., 1989) and PDO-positive conditions (Kirby et al., 2012) but the response to long-term, millennial-scale and glacial–interglacial climate oscillations are topics of debate.

On the scale of glacial cycles, most studies have found that pluvial lakes in the southwestern US reached their highest levels during or somewhat after maximum glacial stages (e.g., Smith et al., 1997; Oviatt et al., 1999; Reheis et al., 2002). The oldest hypothesis suggests that during the last glaciation (marine oxygen-isotope stage [MIS] 2), levels of Great Basin pluvial lakes tracked the north–south migration of the polar jet in response to advance and retreat of the Laurentide ice sheet (e.g., Antevs, 1948; Thompson et al., 1993; Benson et al., 1995). Alternatively, Lyle et al. (2012) proposed that the average position of the jet stream did not move during MIS 2, and that high lake levels migrated from southeast to northwest due to increased incursions of tropical moisture. Recent studies of the southwesternmost lakes suggest they persisted at relatively high levels for longer periods during MIS 3 and 2 and reached highstands earlier than lakes to the north (Owens Lake—summarized in Phillips, 2008; Lake Mojave—Wells et al., 2003; Lake Estancia—Allen and Anderson, 2000; Lake Manix—Reheis et al., 2012).

The behavior of pluvial lakes in the Great Basin during MIS 3 has also been attributed to movement of the polar jet and its associated westerly storm track (Benson et al., 2003, 2011, 2013), as well as to changes in sea-surface temperature (SST; Hendy and Kennett, 2000; Hendy, 2010) and consequent changes in atmospheric moisture. Other explanations include tropical sources of moisture as suggested by Lyle et al. (2012) and Wells et al. (2003) for MIS 2. Denton et al. (2005) proposed that abrupt climate changes such as the Younger Dryas and the

* Corresponding author. Fax: +1 303 236 5349.
E-mail addresses: mreheis@usgs.gov (M.C. Reheis), dmiller@usgs.gov (D.M. Miller), mcgeehin@usgs.gov (J.P. McGeehin), jredwine@usbr.gov (J.R. Redwine), joviatt@k-state.edu (C.G. Oviatt), jbright1@email.arizona.edu (J. Bright).

http://dx.doi.org/10.1016/j.yqres.2014.11.003
0033-5894/ Published by Elsevier Inc. on behalf of University of Washington.

D–O cycles were triggered by expansion of North Atlantic sea ice that shut down the Atlantic meriodional overturning circulation, in turn leading to changes in strength of the Asian monsoon and to movement of the intertropical convergence zone (ITCZ). Such atmospheric reorganization could account for changes in precipitation delivered to the western US.

MIS 3 lake records have been previously studied mainly through proxy data, primarily carbonate $\delta^{18}O$ and inorganic and organic carbon contents measured on lake cores, although some outcrop data for this time frame exists. Several papers (Benson et al., 2003, 2011, 2013; Kirby et al., 2006) concluded that Great Basin lakes—although much lower than during their post-last glacial maximum (LGM) highstands—achieved relatively higher levels during the interstadials (as interpreted from the Greenland ice record; Svensson et al., 2006) of the Dansgaard–Oeschger (D–O) cycles and were low during the stadials. This effect was interpreted to be consistent and synchronous from as far north as Lake Chewaucan in southern Oregon (Benson et al., 2003) and as far south as Baldwin Lake in southern California (Kirby et al., 2006), across 8° of latitude. In contrast, recently published speleothem data from Arizona and New Mexico suggest that local climatic conditions were cool and wet during the D–O stadials rather than interstadials (Asmerom et al., 2010; Wagner et al., 2010). Phillips et al. (1994) interpreted records from Searles Lake to indicate higher lake levels during MIS 3 stadials, and Garcia et al. (2014) interpreted a highstand of Harper Lake about 45–40 ka to indicate a southward (stadial) position of the polar jet.

Obtaining accurate chronometric ages is the major difficulty in deciphering the response of Great Basin lakes to climate change during MIS 3 at the frequency of a D–O cycle (roughly 1500 yr; Schulz, 2002). From 30 to 25 ka, radiocarbon ages may be of sufficient resolution, but older samples have increasing analytical and geologic uncertainties that can exceed a half cycle. Luminescence dating has even greater uncertainties. Lake cores may suffer from errors in age models based on radiocarbon dates on different materials (e.g., bulk carbon vs. shells) that may be influenced by a number of factors, and varying sedimentation rates. Correlation using paleomagnetic secular variation has promise but relies on long-distance correlation to North Atlantic marine records and thence to Greenland ice cores (e.g., Benson et al., 2011, 2013).

In this paper, we studied an MIS 3 record by obtaining ~70 ^{14}C ages on deposits that closely constrain lake levels through sedimentary facies and stratigraphy, and by tracing outcrops across the landscape through facies changes to establish lake-level fluctuations (e.g., Cohen, 2003; Reheis et al., 2014a). We mapped and dated shell-bearing deposits of Lake Manix, in the Mojave Desert of south-central California, to establish a directly dated lake level record that extends from about 45 to 25 cal ka BP. The use of multiple dates on the same stratigraphic units can mitigate, though not eliminate, the issue of accurate and precise ^{14}C ages at least for the latter part of MIS 3 (younger than 40 ka).

Background and setting

Pluvial Lake Manix is the former terminus of the Mojave River, which drains the San Bernardino Mountains and flows to the east and northeast for nearly 200 km across the Mojave Desert (Fig. 1). Reheis et al. (2012) reviewed the climate and discharge records for this area. The vast majority of precipitation in the river basin occurs in the headwaters region (Enzel and Wells, 1997), where the mountains intercept Pacific storms. Rainfall is extremely low in the area of the Manix basin and evaporation rates in the Mojave Desert are >2000 mm yr^{-1} (Blaney, 1957; Enzel, 1992).

The river terminated in Lake Manix from about 500–25 ka (Cox et al., 2003; Reheis et al., 2012), with occasional diversions to the Harper basin

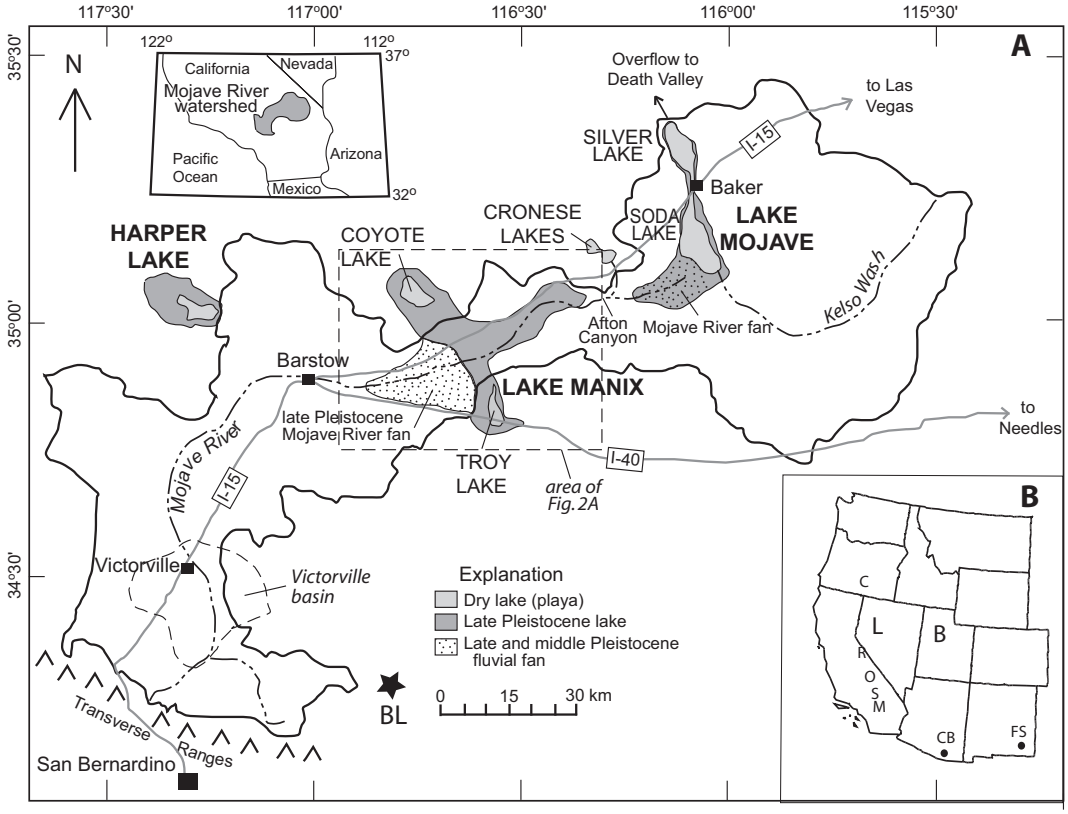

Figure 1. A, map showing late Pleistocene lake basins along the Mojave River. Inset in upper left shows location of drainage basin in southern California. Light gray, extent of modern playa surfaces. Dark gray, extent of late Pleistocene highstands of Harper Lake, Lake Manix, and Lake Mojave. Star labeled BL is location of Baldwin Lake. Modified from Reheis and Redwine (2008) and Jefferson (2003). B, western United States showing locations additional lake and speleothem records. Pluvial lakes: B, Bonneville; C, Chewaucan; L, Lahontan; M, Manix; O, Owens; R, Russell (Mono Lake); S, Searles. Caves: CB, Cave of the Bells; FS, Fort Stanton.

https://doi.org/10.1016/j.yqres.2014.11.003 Published online by Cambridge University Press

(Reynolds and Reynolds, 1994; Meek, 1999; Garcia et al., 2014). Nearshore deposits (Reheis and Redwine, 2008; Reheis et al., 2014b) show that during MIS 6–2, Lake Manix repeatedly reached elevations that would have simultaneously submerged the Afton, Cady, and Troy subbasins and frequently also Coyote subbasin (Fig. 2). At ~25 ka Afton Canyon was incised and Lake Manix drained (Reheis and Redwine, 2008). For the next several thousand years the river alternately fed lakes in the Coyote subbasin and the Cronese and Soda-Silver basins (Fig. 1; Meek, 1999; Enzel et al., 2003; Miller et al., 2009).

As much as 20 m of late Pleistocene lacustrine and interbedded alluvial sediments are exposed along the Mojave River in both Cady and Afton subbasins (Fig. 2; Reheis et al., 2014b). These sediments commonly contain fossil freshwater clams (*Anodonta californiensis*) and locally, aquatic gastropods, that yield reliable radiocarbon ages. Although the Troy and Coyote Lake subbasins have not been deeply dissected, shallow outcrops of nearshore sediment have also yielded *Anodonta*. Due to progressive sedimentation throughout the lake basin during the history of Lake Manix (Reheis et al., 2012) and high evaporation rates as a result of low latitude and altitude, the lake was probably shallow and highly sensitive to climate perturbations.

Methods

We mapped Lake Manix deposits at scales of 1:12,000–1:24,000, measured numerous stratigraphic sections from outcrops and hand-dug pits, and collected shells for dating tied to these sections (Reheis and Redwine, 2008; Miller et al., 2009; Reheis et al., 2014b). Altitudes of most measured sections were obtained using differentially corrected GPS and are considered accurate to within ±1 m. Some altitudes were obtained by estimation from LIDAR data and are probably accurate to within 50 cm.

Dated deposits consist of nearshore lacustrine sediment and, in the area of the Mojave River–Manix Wash confluence (Fig. 1), fluvial and deltaic sediment deposited by the river as it prograded into Lake Manix (Meek, 1990; Jefferson, 2003). The dated deposits represent the youngest lake unit, Ql8 of Reheis et al. (2014b), which is equivalent to

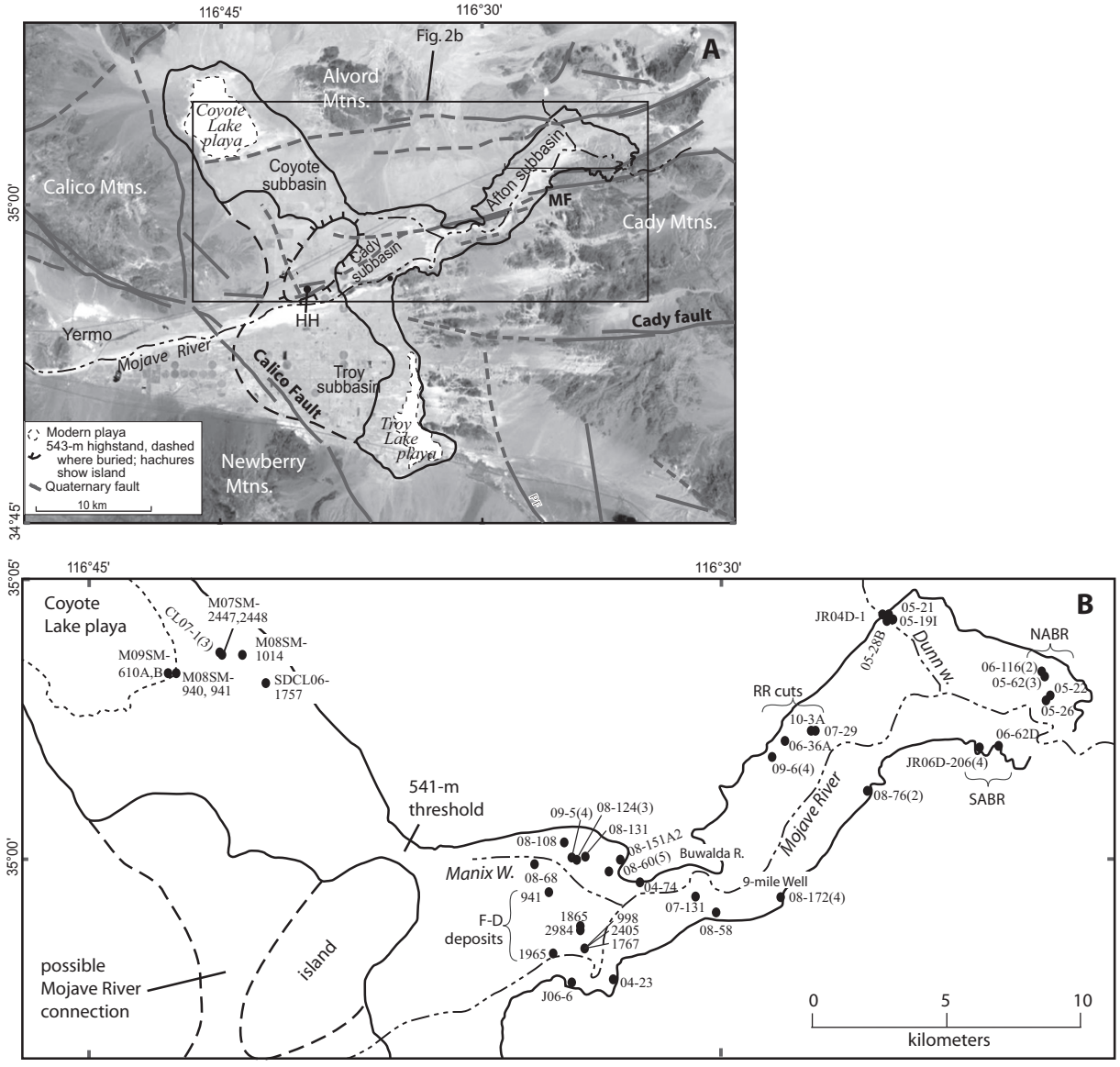

Figure 2. Map of study area. A, geographic features of the Manix basin. Solid black line represents 543-m highstand altitude of Lake Manix (dashed where buried). Dash-dot lines are drainages of Mojave River, Manix Wash, and Dunn wash (informal name). MF, Manix fault zone. HH, Harvard Hill. Modified from Reheis and Redwine (2008). B, detail showing dated *Anodonta* sample sites. Sample numbers and measured sections have been abbreviated for convenience from longer names given in Table 1 by removing letter and year prefixes, except for J06-6, JR06D-1, JR06D-206, and samples from core CL07. Parentheses give number of dated samples at sites with multiple fossil layers. NABR and SABR, North Afton and South Afton beach ridges; F-D, fluvial–deltaic deposits.

https://doi.org/10.1016/j.yqres.2014.11.003 Published online by Cambridge University Press

"member D" of Jefferson (2003). In the Afton and Cady subbasins, this unit commonly consists of multiple transgressive–regressive packages of lacustrine sediment. The packages are typically separated in outcrop by layers of clasts coated with tufa deposited during transgressions, and locally by intervening thin (commonly <50 cm thick) alluvial-fan deposits with buried soils. By physically tracing these packages or subunits along arroyo cuts that are perpendicular to the shoreline, the upper and lower altitude limits of each subunit can be defined in a particular drainage or area. These altitudes are considered minimum estimates of lake level because thin deposits of nearshore lake sediment from a given cycle could have been eroded prior to the next transgression. The records from each area can then be correlated on the basis of their ^{14}C ages to assemble a coherent lake-level record for the lake. ^{14}C-dated deltaic deposits are so variable in character, due to fluctuating lake depth and laterally migrating channels (Reheis and Miller, 2010) that they cannot easily be used to reconstruct lake-level changes. However, dated deltaic deposits do provide supporting evidence that the river was entering the lake at a given time.

In the Coyote subbasin (Fig. 2) we studied the few arroyo exposures using methods similar to those for the other subbasins. We also evaluated provenance in the sediment sequences using the distinction between local sediment sources of meta-granitic and volcanic rocks, in contrast to the quartzite and granite of the Mojave River sediments. This allowed us to recognize at least one episode of Mojave River sediment delivered to Coyote before the demise of Lake Manix.

Most ^{14}C ages were measured on freshwater *Anodonta* that today live exclusively in shallow water of lakes and streams, generally less than 2 m deep (Ingram, 1948). Thus, their presence in lacustrine deposits documents lake level to within ~2 m, assuming they were not reworked far downslope through wave action. To mitigate this possibility, we mainly restricted samples to whole shells or valves; in a few cases, we sampled concentrations of large shell fragments. Although this mollusk was endemic in the Mojave River and its (ephemeral) lakes up to historic time, it is now extirpated in the study area. *Anodonta* shells are dominantly composed of aragonite (e.g., Borbas et al., 1991; Lopes-Lima et al., 2010), particularly the inner nacreous layer that composes 90% of the shell thickness, but the mineralogic composition of the thin (<0.1 mm) outer prismatic layer had not been previously determined on *A. californiensis*. We obtained modern shells and used a burring drill under a binocular microscope to sample this outer layer. X-ray diffraction analysis indicated that the prismatic layer was mainly composed of aragonite but a small component of calcite was present. Therefore, the presence of calcite in a shell sampled for dating could either indicate replacement by younger carbon after deposition, or preservation of the thin outer layer.

Radiocarbon ages were obtained from lacustrine deposits of the youngest phase of Lake Manix; 50 of these were from the main Afton and Cady subbasins and 11 from the Coyote subbasin (Table 1). Seven ages are reported from the fluvial–deltaic deposits equivalent to Ql8. Samples were processed at the ^{14}C laboratory of the U.S. Geological Survey in Reston, Virginia, and ages were determined at the Center for Accelerator Mass Spectrometry (CAMS), Lawrence Livermore National Laboratory, Livermore, California. In addition, one age was on aquatic gastropods (*Valvata utahensis*) and several ages were obtained on ostracodes picked from samples of cores drilled in the Soda Lake subbasin of Lake Mojave, downstream of Lake Manix (Fig. 1), in the 1950s (Muessig et al., 1957). Two of these ages (SL-830-Lb and SL-860-Lb from the Soda-1 core) were reported in Reheis and Redwine (2008); here we report three additional ages from the bases of the Soda-1 and Soda-3 cores (Table 1) to constrain the timing of the last highstand of Lake Manix and the first arrival of water in Lake Mojave.

Shells and shell fragments were isolated by soaking samples in a weak Calgon solution for several hours. The shells were sonicated in distilled water for 1 h to remove additional surface sediment. In certain cases, when the shell material was still encrusted in sediment or showed signs of surface alteration, the sample was soaked in dilute (0.1 M) HCl to etch the surfaces clean. Despite this treatment, the older samples in particular may have been contaminated by young carbon (Zimmerman et al., 2012), yielding ages that are systematically too young. We subtracted 140 years from all ages, including those of the aquatic gastropod and ostracodes, to adjust for estimated content of old carbon as determined by Miller et al. (2010) on paired dates from *Anodonta* shells and charcoal from Holocene deposits in the nearby Cronese basins (Fig. 1). Most samples were also analyzed for ^{13}C and the reported ^{14}C ages are accordingly corrected with δ^{13}C values. For samples lacking δ^{13}C values (analyzed prior to 2007), we used the average δ^{13}C value measured on all other samples (-4 ± 2‰). The quoted age is in radiocarbon years using the Libby half-life of 5568 years. Results were converted to calibrated years (cal yr BP) using the IntCal13 dataset and CALIB 7.0 (Stuiver and Reimer, 1993; Reimer et al., 2013). We note that in the time range of interest here, the use of IntCal13 yields calibrated ages as much as 700 yr younger than by using IntCal09 (Reimer et al., 2009). The calibrated ages and uncertainties shown in Table 1 are the peak mode and 2σ error range, respectively.

Nearly all of the ages within a given section are in stratigraphic order within analytical error, with only two exceptions, both located on the east side of Manix Wash (Fig. 2): M08-60c and M09-5. The two lowest dates from M08-60c are in stratigraphic order, but the two uppermost dates are significantly older, despite the fact that M08-60c2 and -60c3 are from the same depositional package with no hiatus separating them. We resampled a shell from M08-60c3 and replicated the discrepant age. Of the four samples, the two lowest and youngest are from continuous concentrations of many entire valves, suggesting little or no reworking. We analyzed shells from these same two beds using XRD and found that M08-60c1 contained only aragonite and M08-60c2 contained a trace of calcite, possibly due to inadequate cleaning of the shell (the remaining sample after dating was too small to treat with HCl and still X-ray). In contrast, the two highest and oldest samples are from scattered valves and large shell fragments. Thus, it is possible that the two uppermost samples, M08-60c3 and -60c4, were reworked from older shell beds in the vicinity. At the other site with discrepant ages, M09-5, we dated samples from four units. The upper two samples, JO-17 and M09-5, yielded ages in stratigraphic order. The age of the next lower sample, JO-16, although slightly younger than M09-5, overlaps it within analytical error, and these two samples are not separated by an obvious hiatus or buried soil. Shell material from M09-5 contained only aragonite; we had no remaining shell from the other samples for testing. The lowest age, JO-15, is significantly younger than the overlying samples but is separated from them by a brown mud and buried soil. We traced this depositional unit to the southeast, where it pinches out and the overlying soil merges with an unconformity and buried soil formed on the next older lake unit, Ql7. We interpret the discrepant age to be caused by replacement by younger carbonate in a paleo-weathering environment.

Results

Shell samples from Lake Manix are mainly derived from the Afton and Cady subbasins, which were contiguous during the late Pleistocene. A subset of samples are from the Coyote subbasin, which was probably separated from the main body of Lake Manix during this time by a thick wedge of older fluvial–deltaic deposits present today in the subsurface between the Calico Mountains and Harvard Hill (Fig. 2). Thus, the connection to the Coyote subbasin during most of the late Pleistocene is a bedrock sill at an altitude of about 541 m above sea level (masl) near the head of Manix Wash. Because the highstand of Lake Manix during late Pleistocene time was at about 543 masl, the Coyote subbasin served as a threshold control that stabilized lake level; spillage over this threshold greatly expanded the lake area and consequently evaporation (Meek, 1994). The presence of lake deposits—regardless of their altitude—in the Coyote subbasin of the same age as deposits in the

https://doi.org/10.1016/j.yqres.2014.11.003 Published online by Cambridge University Press

Table 1
Radiocarbon samples, locations, and age data.

Station	Lab no. [a]	Easting	Northing	Altitude (m) [b]	^{14}C age[c]	Std. dev.	δ^{13}C [d]	^{14}C (corr.) [e]	INTCAL13 peak mode [f]	Lower bound	Upper bound	Description [g]
Afton subbasin samples												
JR04D-1	WW4924	551349	3880423	**541.0**	25,390*	110	n.d.	25,250	29,298	28,966	29,610	Foreshore of 543-m beach ridge; see Fig. 4
M05-21	WW5629	551474	3880398	**535.4**	31,870*	230	n.d.	31,730	35,622	35,076	36,145	Large shell fragments; see Fig. 4
M05-28B	WW5343	551395	3880292	**532.2**	26,000*	100	n.d.	25,860	30,091	29,665	30,512	Back-barrier playa setting; see Fig. 4
M05-19I	WW5340	551614	3880174	**526.0**	34,650*	260	n.d.	34,510	39,012	38,478	39,644	Large shell fragments. See Fig. 4; unit traced to at least 536 masl
M05-22H	WW5341	557663	3878175	**539.4**	26,960*	120	n.d.	26,820	30,966	30,761	31,157	Sample is from very top of beach ridge; see Fig. 7
M05-26G	WW5632	557501	3878054	**532.3**	29,590*	190	n.d.	29,450	33,660	33,229	34,011	*Anodonta* mixed with fish bones and snails just below buried soil
M05-62A	WW7485	557377	3878879	**533.2**	30,600	240	−3.7	30,460	34,431	33,993	34,855	Large shell fragment. See Fig. 7
M05-62	WW5633	557377	3878879	**533.8**	28,410*	160	n.d.	28,270	32,129	31,573	32,724	Shell reef. See Fig. 7
M05-62C	WW7486	557377	3878879	**534.0**	26,620	150	−4.9	26,480	30,769	30,460	31,028	See Fig. 7
M06-116A	WW6070	557305	3879041	**533.1**	21,140	70	−1.9	21,000	25,357	25,132	25,571	Small rise on foreslope of North Afton beach ridge. May represent temporary stabilization during downcutting
M06-116B	WW6070	557305	3879041	**533.6**	20,510	70	−4.9	20,370	24,456	24,208	24,808	Small rise on foreslope of North Afton beach ridge. May represent temporary stabilization during downcutting
JR06D-206C1	WW5881	555095	3876179	*534.3*	26,590*	90	n.d.	26,450	30,762	30,540	30,977	Shell reef, growth position. See Fig. 7
JR06D-206E	WW7483	555095	3876179	*535.1*	23,140	100	−4.9	23,000	27,334	27,102	27,538	See Fig. 7
JR06D-206 F	WW7484	555095	3876179	*535.3*	21,780	80	−3.0	21,640	25,909	25,752	26,068	Redate of JR06D-206B. Shell in growth position. See Fig. 7
JR06D-206A	WW5879	555095	3876179	*536.3*	21,800*	60	n.d.	21,660	25,923	25,788	26,062	See Fig. 7
M06-62D	WW5885	555809	3876066	**538.6**	21,280*	50	n.d.	21,140	25,493	25,273	25,671	Overlies Bwk on dune? sand; grades up to 543-m crest of south Afton beach ridge
M07-29	WW6343	548966	3876489	**522.6**	36,040	400	−7.0	35,900	40,529	39,647	41,384	See Fig. 7
M10-3A	WW8115	548886	3876488	522	36,410	300	−6.2	36,270	40,912	40,229	41,526	Abundant snails, *Valvata utahensis*. See Fig. 7
M07-36A	WW6344	547891	3876226	**533.0**	27,070	140	−2.8	26,930	31,019	30,805	31,218	Large shell fragments. See fig. 7
M09-6A	WW7617	547480	3875665	**533.0**	39,280	770	−5.7	39,140	43,021	41,955	44,319	See Fig. 7
M04-74	WW5279	547480	3875665	**535**	28,140*	120	n.d.	28,000	31,701	31,362	32,224	Shell reef; bed has S-dipping foresets. See Fig. 7
M09-6B	WW7491	547480	3875665	**534.4**	27,810	170	−3.1	27,670	31,417	31,133	31,766	See Fig. 7
M06-89	WW5886	547480	3875665	**535.3**	23,100*	70	n.d.	22,960	27,308	27,105	27,487	See Fig. 7
M08-58	WW6986	545652	3869849	**542.4**	21,450	70	−4.1	21,310	25,661	25,466	25,844	Large shell fragments. Small beach ridge S of river surmounts high fan surface, sampled ~1 m below top
M08-76A	WW7109	550538	3874023	**524.0**	26,790	230	−5.9	26,650	30,860	30,469	31,173	Base of Ql8; faulted locality south of river
M08-76B	WW7110	550538	3874023	**529.0**	21,980	120	−1.8	21,840	26,058	25,836	26,347	Unit Ql8; faulted locality south of river
M08-172A	WW8041	547942	3870478	**533.5**	27,920	190	−6.7	27,780	31,513	31,155	32,027	See Fig. 7
M08-172C	WW8042	547942	3870478	**534.9**	24,400	120	−4.4	24,260	28,298	27,962	28,626	See Fig. 7
M08-172D	WW8043	547942	3870478	**536.7**	23,200	100	−3.0	23,060	27,378	27,149	27,583	See Fig. 7
M08-172	WW7496	547942	3870478	**536.7**	23,120	100	−3.7	22,980	27,319	27,088	27,524	See Fig. 7
Cady subbasin samples												
M07-131	WW6346	544793	3870134	537.2	26,860	140	−5.3	26,720	30,914	30,689	31,123	South side of river
M04-23	WW4771	542031	3867455	539.0	21,750*	60	n.d.	21,610	25,890	25,750	26,033	S side river. In highest of 3 fining-upward Ql8 units, capped by weak soil and eolian sand
J06-6	WW7233	540030	3867210	539.0	21,320	80	−5.2	21,180	25,532	25,276	25,737	South side of river. Highest of 2 Ql8 units capped by regression gravel / fan gravel
M04-75	WW5357	542357	3871122	**542**	22,430*	70	n.d.	22,290	26,521	26,219	26,876	See Fig. 7
M08-60c-1	WW6987	541287	3871190	**531.3**	31,510	230	−5.0	31,370	35,249	34,752	35,774	Whole shells. See Fig. 7
M08-60c-2	WW6988	541287	3871190	**531.8**	24,400	130	−4.2	24,260	28,297	27,949	28,635	Whole shells. See Fig. 7
M08-60c-3	WW7616	541287	3871190	**532.0**	34,970	450	−3.8	34,830	39,359	38,450	40,355	Scattered valves; age reversal. See Fig. 7
M08-60c-3 resample	WW8113	541287	3871190	**532.0**	33,320	210	−5.2	33,180	37,377	36,621	38,204	Scattered valves; resampled to check age. See Fig. 7
M08-60c-4	WW8114	541287	3871190	**533.0**	32,710	190	−5.2	32,570	36,469	35,993	37,062	Large shell fragments; age reversal. See Fig. 7
J06-15	WW7112	540611	3871782	**529.9**	33,410	490	−2.9	33,270	37,484	36,269	38,632	Weathered valves; age reversal, Fig. 7
J06-16	WW7113	540611	3871782	**530.6**	34,410	580	−3.9	34,270	38,745	37,033	40,073	Weathered valves; age reversal, Fig. 7
M09-5	WW7492	540611	3871782	**531.3**	35,980	450	−5.2	35,840	40,461	39,468	41,415	See Fig. 7
J06-17	WW5850	540611	3871782	**532.5**	31,880*	330	n.d.	31,740	35,625	34,927	36,283	See Fig. 7
M08-124A	WW7202	540800	3871758	531.0	29,610	130	−2.6	29,470	33,689	33,417	33,949	See Fig. 7
M08-124	WW8116	540800	3871758	532.6	29,090	190	−5.3	28,950	33,158	32,610	33,651	See Fig. 7
M08-124C	WW8117	540800	3871758	532.7	27,430	130	−6.6	27,290	31,195	31,000	31,395	See Fig. 7
M08-141	WW7108	541141	3871845	531.5	34,600	570	−2.6	34,460	38,976	37,421	40,323	Large shell fragments. Soil ~15 cm below shell layer
M08-108	WW7201	540315	3872581	535.7	28,230	190	−4.7	28,090	31,886	31,393	32,571	2 m interbedded sand and gravel of Ql8 overlies Ql7, shells in two beds; samples from basal bed
M07-151A2	WW6345	541941	3871764	**539.5**	21,580	70	−3.6	21,440	25,765	25,597	25,923	Beach sand and gravel of unit Ql8, 75 cm below surface; overlies weak soil formed on older Ql8 bed
M08-68B	WW6989	539877	3871666	**528.2**	37,320	440	−5.9	37,180	4,1670	40,893	42,333	See Fig. 7
Fluvial–deltaic samples from Manix Wash-Mojave River confluence												
M06NS-941	WW5716	539291	3870382	*527.3*	39,970*	610	n.d.	39,830	43,530	42,595	44,582	Isolated site. See Fig. 5
M06NS-1865	WW5849	540615	3869575	*530.5*	34,890*	460	n.d.	34,750	39,281	38,368	40,318	North of Manix core site. See Fig. 5
M05NS-2984	WW5518	540625	3869416	*532.9*	32,100*	240	n.d.	31,960	35,857	35,292	36,349	North of Manix core site

(continued on next page)

https://doi.org/10.1016/j.yqres.2014.11.003 Published online by Cambridge University Press

Table 1 *(continued)*

Station	Lab no. [a]	Easting	Northing	Altitude (m) [b]	^{14}C age[c]	Std. dev.	δ^{13}C [d]	^{14}C (corr.) [e]	INTCAL13 peak mode [f]	Lower bound	Upper bound	Description [g]
Fluvial–deltaic samples from Manix Wash-Mojave River confluence												
M05NS-1965	WW5356	539542	3868485	*533.8*	31,990*	190	n.d.	31,850	35,755	35,277	36,197	West of Manix core site. See Fig. 5
M03NS-1767	WW4564	540726	3868771	*534.7*	29,010*	170	n.d.	28,870	33,068	32,530	33,566	South of Manix core site. See Fig. 5
M06NS-2405	WW6062	540751	3868790	*535.8*	26,270	160	−3.8	26,130	30,443	29,883	30,828	South of Manix core site. See Fig. 5
M09NS-998	WW7376	540717	3868778	*536.6*	25,540*	90	n.d.	25,400	29,474	29,166	29,781	South of Manix core site. See Fig. 5
Coyote subbasin samples												
CL07-1B-14 cm	WW6543	527290	3879319	524.9	30,120*	390	−2.9	29,980	34,071	33,421	34,762	Shell fragments. Coyote core site; see Fig. 6
08CL-1B-35 cm	WW7111	527290	3879319	524.9	38,330	900	−3.8	38,190	42,333	40,869	43,772	Massive mud. Coyote core site; see Fig. 6
CL07-1D-3	WW7234	527290	3879319	522.3	45,120	1370	−4.2	44,980	48,098	45,944	50,000	Coyote core site
M07SM-2447	WW6544	527330	3879269	525	42,400	1600	−6.0	42,260	45,695	42,929	48,838	Lower sample near Coyote core site; see Fig. 6
M07SM-2448	WW6545	527372	3879233	525	31,300	420	−2.8	31,160	35,084	34,282	35,954	Upper sample near Coyote core site; see Fig. 6
M08SM-1014	WW7435	527772	3879297	528.9	29,870	280	−1.5	29,730	33,867	33,362	34,398	SE Coyote higher section; see Fig. 6
M08SM-940	WW7433	526258	3878593	520	31,850	360	−4.3	31,710	35,595	34,856	36,300	Coyote south platform upper bed; receding lake
M08SM-941	WW7434	526297	3878605	520	34,270	480	−3.8	34,130	38,594	37,119	39,744	Coyote south platform lower bed; receding lake
M09SM-610A	WW7373	526144	3878608	524.1	32,870	230	−2.4	32,730	36,689	36,128	37,569	Coyote wash cut, regressive sand
M09SM-610B	WW7374	526144	3878608	524.2	32,690	210	−7.2	32,550	36,455	35,916	37,113	Coyote wash cut, blocky muddy sand on sand
SDCL06-1757	WW5712	528541	3877714	533.5	22,450*	170	n.d.	22,310	26,575	26,133	27,077	SE Coyote, youngest full Manix deposits
Soda Lake core samples												
SL-830-Lb	WW4872	USGS Soda-1 core		n.d.	18,010*	70	n.d.	17,870	21,659	21,415	21,876	Ostracodes, 25.3 m depth
SL-860-Lb	WW4873	USGS Soda-1 core		n.d.	18,750*	60	n.d.	18,610	22,470	22,345	22,628	Ostracodes, 26.2 m depth
Soda1-106 ft	WW8005	USGS Soda-1 core		n.d.	20,510*	150	n.d.	20,370	24,494	24,084	25,011	Ostracodes, 32.3 m depth
Soda3-115 ft	WW8006	USGS Soda-3 core		n.d.	21,590*	100	n.d.	21,450	25,770	25,563	25,960	Ostracodes, 35.0 m depth
Soda3-124 ft	WW8007	USGS Soda-3 core		n.d.	20,740*	250	n.d.	20,600	24,809	24,174	25,454	Ostracodes, 37.8 m depth

* Asterisk following ^{14}C age indicates δ^{13}C value not measured in laboratory.

[a] Samples were pretreated at the ^{14}C laboratory of the U.S. Geological Survey in Reston, Virginia.

[b] Bold font indicates differentially corrected GPS data; altitudes in normal font estimated from topographic map and handheld GPS. Italic font indicates altitudes from NASA ATM-III LIDAR data acquired September, 2004, funded by the U.S. Army Corps of Engineers, WRAP program R. Lichvar & D. Finnegan.

[c] ^{14}C ages were determined at the Center for Accelerator Mass Spectrometry (CAMS), Lawrence Livermore National Laboratory, Livermore, California. Quoted age is in radiocarbon years (B.P.) using Libby half-life of 5568 yr, corrected for measured or estimated δ^{13}C value.

[d] δ^{13}C measured on all samples beginning in 2007. Average ^{13}C value of 4.0 used for samples not measured, calculated from all measured Anodonta samples.

[e] Ages corrected for reservoir age of ~ −140 yr (Miller et al., 2010).

[f] Calibration performed using Calib v. 7.0 (http://calib.qub.ac.uk/calib/) accessed November 2013. Peak mode as listed in program output.

[g] All analyses performed on *Anodonta californiensis* shells except for M10-3A and Soda Lake core samples; samples are whole valves unless noted.

main subbasins thus indicates that lake level at that time in the main subbasins equaled or exceeded 541 masl. At times that lake level was below 541 m, the Mojave River sometimes fed the Coyote subbasin directly, so Coyote subbasin ages may not always match highstands in other subbasins. The key evidence for direct Mojave River introduction to Coyote Lake is fluvial deposits of the Mojave River reworked into lacustrine sand, as opposed to locally derived sand.

Site stratigraphy

Depositional environments of the sediments in the dated measured sections ranged from beach sand and gravel in the Afton and Cady subbasins to mud and sand of fluvial–deltaic deposits west of Manix Wash to nearshore fine to muddy sand in the Coyote subbasin. Following are examples that illustrate these environments and their relation to lake level. Most of the dating sites are shown in Figs. 3–7; see Reheis et al. (2014b) for details of additional sections that are not portrayed.

Beach deposits, Section M05-62, Afton subbasin

Section M05-62 is 3 m thick and lies on the lakeward side of the North Afton beach ridge (Figs. 2 and 3). Like many beach deposits in this basin, it is composed of arkosic sand and pebble to cobble gravel arranged in 25–50-cm-thick packages or units, some of which fine upward. Bedding dips range from horizontal to 5–15° lakeward or shoreward, typical of deposition in beach barriers. Each unit is usually abruptly overlain by a distinct line of clasts with very thin tufa coats that marks the next younger transgression phase. The tufa coats are interpreted to represent deposition of $CaCO_3$ in the swash zone, possibly due to incorporation of carbonate-rich eolian dust deposited during the previous lake regression. The upper few cm of each unit may be weakly oxidized and (or) cemented with calcium carbonate, suggesting aerial exposure. Although somewhat subjective, we define a unit as bounded by a transgressive basal gravel and an abrupt upward termination marked by such oxidation or cementation; some units may contain one or more tufa-coat lines suggesting rapid lake-level fluctuations. In this section, there are at least five units representing distinct lake cycles that are separated by lake regression and surface exposure. Samples from three units yielded ages in stratigraphic order ranging from 34,860–33,990 to 31,030–30,460 cal yr BP. Each dated level is separated by about 2000 yr.

Fan-lake interface deposits, upper Dunn wash, Afton subbasin

Sediments in upper Dunn wash (informal name; Fig. 2) represent deposition at the margin of an active alluvial fan. As discussed in Reheis and Miller (2010), these are very dynamic environments due to lateral shifts in the fan channel, ephemeral runoff, and rapid lake-level fluctuations. Although the sediments commonly resemble clast-supported alluvial-fan deposits, many beds have been modified by lacustrine processes (e.g., beach foreset and backset beds) and contain *Anodonta* shells and ostracodes. Several measured sections record at least four lake units overlying older alluvial-fan (Qia7) and lake (Ql7) deposits (Fig. 6). The sections are correlated by physically tracing units bounded by buried soils and correlation of ^{14}C ages for about 0.5 km upstream through 13 m of altitude change. Four ages of samples from three units are in stratigraphic order and range from 39,640–38,480 to 29,610–28,970 cal yr BP.

Fluvial–deltaic deposits, west of Manix Wash, Cady subbasin

Fluvial–deltaic sediments equivalent to Ql8 ("Member D" of Jefferson, 2003) represent deposition at the junction of the perennial Mojave River and Lake Manix and compose the uppermost 8–10 m of outcrop north of the Mojave River and west of Manix Wash (Fig. 2). The sediments include channel-fill sand and pebble gravel, crevasse-splay deposits, overbank mud and sand, and planar- to ripple-bedded, thin, well-sorted

https://doi.org/10.1016/j.yqres.2014.11.003 Published online by Cambridge University Press

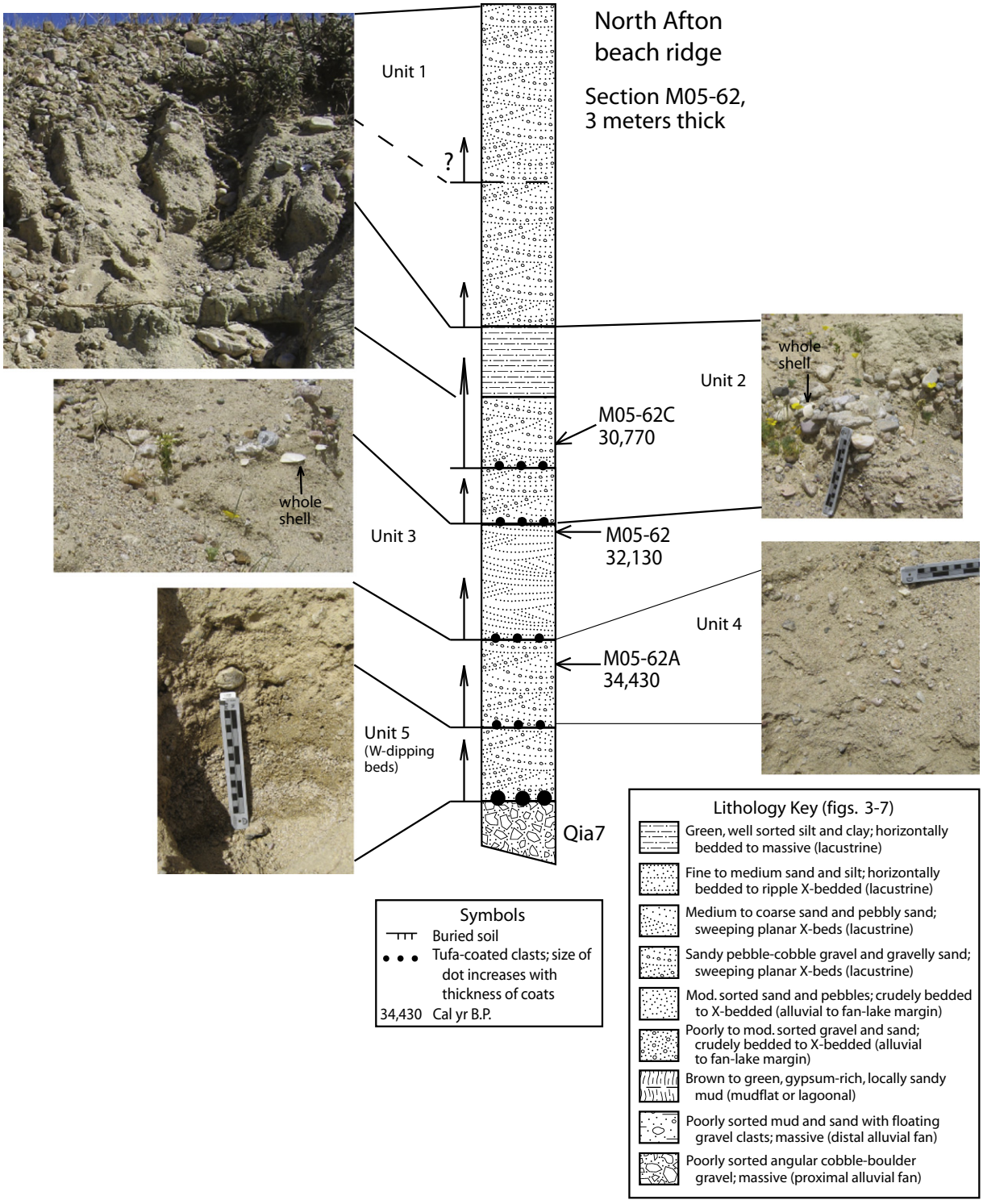

Figure 3. Stratigraphic section and photographs of beach deposits showing sediments, sample locations, and calibrated ^{14}C ages (ranges not shown in Figs. 3–7 for convenience in drafting) at site M05-62 on North Afton beach ridge. Units denoted by number and arrows indicating lake transgression. See Fig. 2 and Table 1 for additional information.

lacustrine deposits (Fig. 5; Reheis and Miller, 2010). Both fluvial and lacustrine beds contain abundant *Anodonta* shells, as well as freshwater snails and turtle remains (Jefferson, 2003), but only *Anodonta* were dated. The ages are in chronologic order with height of the sampled stratum above a distinct contact with the underlying grayish-green muds of lake unit Ql7 (Reheis et al., 2012) and range from 44,580–42,600 to 29,780–29,170 cal yr BP. The two oldest ages are supported by the identification of the 40.7-ka Laschamp magnetic excursion in correlative sediment of the nearby Manix core (Reheis et al., 2012). The deposits are interpreted to represent mainly fluvial aggradation, with temporary transitions to a fluvial-dominated delta on a gently sloping lake margin with shallow lake depth (Reheis and Miller, 2010). Therefore, the dated strata (Fig. 5) record progressive aggradation of sediment deposited by the Mojave River at or near the lake margin from about 45–25 cal ka BP (Reheis et al., 2012), but do not closely constrain lake level.

https://doi.org/10.1016/j.yqres.2014.11.003 Published online by Cambridge University Press

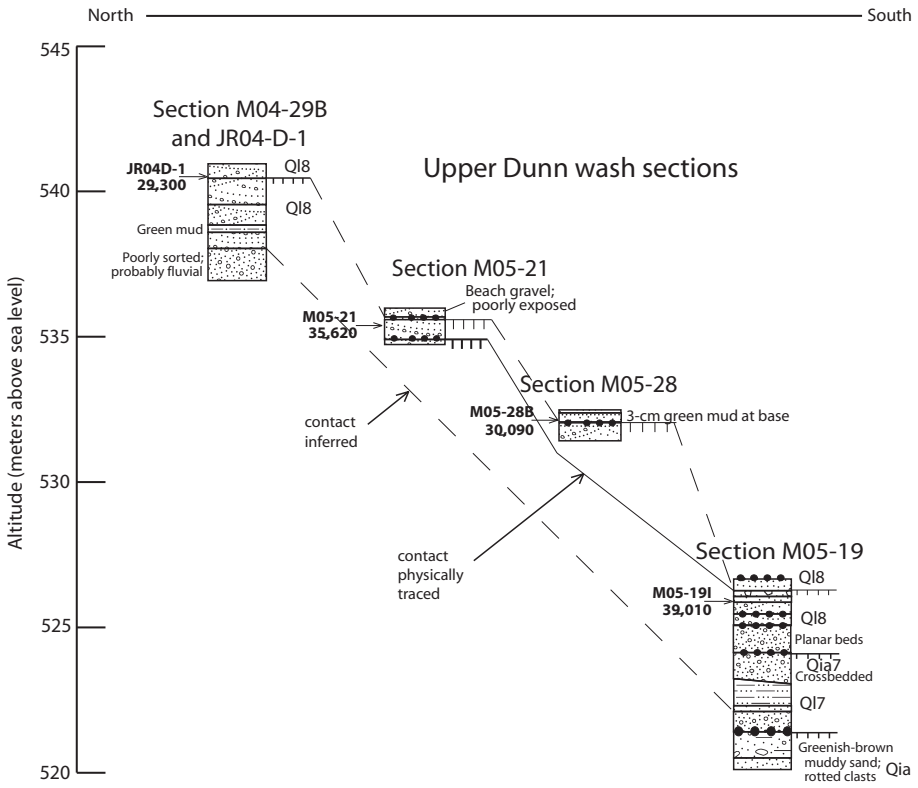

Figure 4. Stratigraphic sections and calibrated ages relative to altitude and distance in fan-lake interface deposits along upper Dunn wash. Hachured lines represent soils, with line weight proportional to degree of soil development. Lithology key same as Fig. 3. See Fig. 2 and Table 1 for additional information.

Nearshore and mudflat sediments, southeastern Coyote subbasin

Exposures of interbedded beach and mudflat deposits in the Coyote subbasin range from near the playa floor (~524 masl) up to the 543-m late Pleistocene highstand of Lake Manix. Incision by local drainages is minor and there is no external drainage; thus, stratigraphic sequences should be relatively continuous except where strata may have been removed by deflation during periods of desiccation. The primary sections related to Lake Manix are exposed on the southern side of the subbasin (Fig. 2). Deposits consist of interbedded cross-laminated to ripple-laminated medium to coarse sand, commonly fining up to muddy fine sand and sandy mud, usually in packages ≤50 cm thick (Fig. 6). The sandy mud and muddy sand beds are commonly oxidized, have soil structure, and locally preserve mudcracks, charcoal flecks, and leaf impressions. These sequences are interpreted as nearshore deposits transitioning upward to sandflat and mudflat deposits caused by episodic incursions of lake water from the main Manix basin to the south. Both muddy and sandy beds contain *Anodonta* shells that yielded 11 ages in stratigraphic order ranging from 50,000–45,940 to 27,080–26,130 cal yr BP. Although the oldest two ages are near the practical limit of radiocarbon dating, their ages are consistent with being separated by buried soils from overlying ages of about 35,000–34,000 cal yr BP. (Fig. 6). The presence of *Anodonta* shells in Coyote sediment during the late Pleistocene requires either that Lake Manix to the south was high enough to exceed the 541-m bedrock threshold required to spill into the subbasin, or that the Mojave River fed directly into the Coyote subbasin; neither case requires the Coyote lake level to reach equilibration with lake level to the south.

Construction of lake-level curve and potential errors

The Manix lake-level curve was constructed through an iterative process. In the first major step, dated strata and lake units in each outcrop were evaluated and correlated across the basin. Each dated outcrop in the Cady and Afton subbasins was closely examined to identify all lake units bounded by a transgressive basal gravel and an abrupt upward termination marked by oxidation or cementation indicating lake regression and exposure. Lake units were physically traced between closely spaced exposures using distinctive beds and buried soils in areas of relatively continuous outcrop, such as sections in upper Dunn wash (Figs. 2 and 3), the two railroad cuts in Afton subbasin, and sections on the east side of Manix Wash (Fig. 7). Dated units were also traced upslope as far as possible to provide a minimum upper bound on lake level represented by each unit. Strongly tufa-coated alluvial fan deposits (Qia7) or a well-developed soil formed on the older Ql7 lake unit provided a consistent base for the Ql8 sequences. Then, the sections were assembled into coherent plots (Figs. 4 and 7) that permitted preliminary correlations among units of similar age, taking into consideration the number of units between ^{14}C ages in each section and buried soils that mark hiatuses. Discrepancies in unit correlations and ages were identified, which led to revisiting outcrops and sometimes revision of units or collection of additional shells for dating.

In the next major step, the calibrated radiocarbon dates were plotted with respect to altitude (Fig. 8). In this plot, the symbols for the dates are coded to indicate groups of dates from the same measured section or closely spaced sections to assess stratigraphic consistency. The three suspect ages (M08-60c3, M08-60c4, and J06-15; not shown in Fig. 8) were not included. We also plotted the ages obtained from the fluviodeltaic deposits west of Manix Wash, which record times when the Mojave River was flowing into a nearby Lake Manix but not the exact lake level. Then we added ages from the Coyote subbasin, which record times when the main lake basin was spilling over the 541-m threshold or the Mojave River led directly to Coyote. Finally, we added ostracode ^{14}C ages from cores taken in Soda Lake (Lake Mojave) downstream, which record the abandonment of the main Manix basin and incision of Afton Canyon (Reheis and Redwine, 2008).

The last major step was to construct a lake-level curve (Fig. 8) that incorporated calibrated ages and altitudes, correlations among units in multiple measured sections, presence of buried soils (red lines)

https://doi.org/10.1016/j.yqres.2014.11.003 Published online by Cambridge University Press

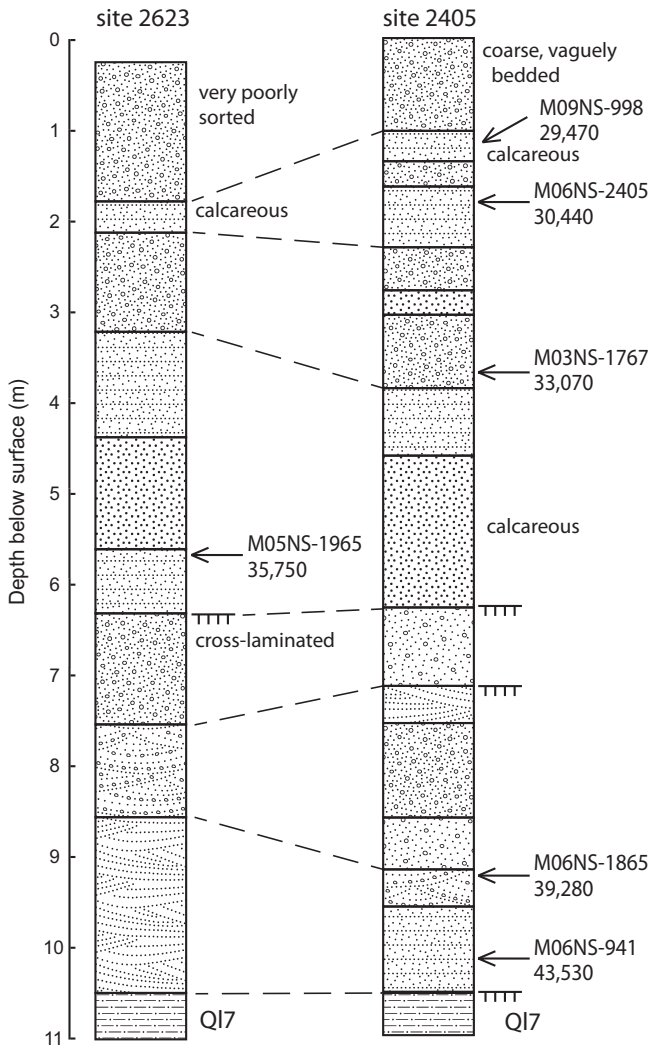

Figure 5. Stratigraphic sections and calibrated ages of fluvial–deltaic sediments near the confluence of Manix Wash and the Mojave River. Samples M06NS-1865 and M06NS-941 are projected from other sections based on height above contact with gray laminated mud (Ql7). Hachured lines represent weak soils. Lithology key same as Fig. 3. See Fig. 2 and Table 1 for additional information. Modified from Reheis et al. (2012).

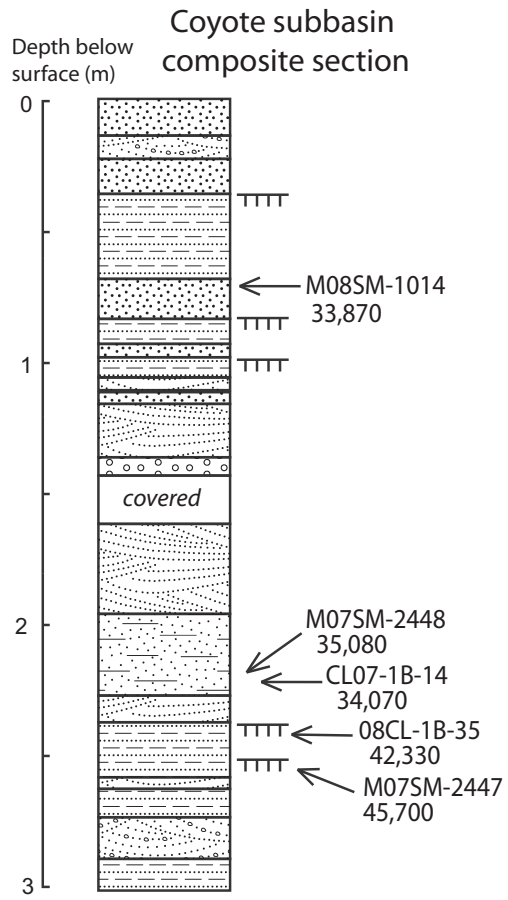

Figure 6. Composite stratigraphic section and calibrated ages of nearshore and mudflat sediments from several closely spaced sites in southeastern Coyote Lake subbasin, including core CL07-1B, a site later hand-dug that yielded additional sample (08CL07-1B). Lithology key same as Fig. 3. See Fig. 2 and Table 1 for additional information.

overlying certain units, and altitudes to which individual units and soils were traced (solid lines). When dated units in the Coyote subbasin matched highstands to the south, we assumed overflow into the Coyote subbasin and upwardly dashed the lake-level curve to 541 masl. Lower dashed bounds of lake level are uncertain due to erosion of sediment along the basin axis by the Mojave River, but we assumed that the basin floor would gradually rise due to sedimentation. Thin dashed lines indicate possible minor lake-level fluctuations not bounded by soils or constrained by only one or two dates. We ensured that the lake-level curve was internally consistent with the numbers of units in each measured section (that is, one or more lake cycles might be missing, but a section could not have more units than lake cycles during a given time interval). The shapes of the curves are somewhat subjective; we assumed that rises in lake level would occur more gradually than falls, as suggested by studies on other well-dated pluvial lakes (Oviatt, 1997; Bacon et al., 2006; Benson et al., 2013). Fig. 8 also shows two dated lake deposits older than 45 ka as well as the interpreted age range for inundation of Lake Harper (Garcia et al., 2014), but we do not include these lake events in our interpretive lake-level curve because of the large analytical uncertainty. One Coyote subbasin shell (M07SM-2447) dated at about 46 cal ka BP lies in lake sediment stratigraphically below ~42 cal ka BP sediments, separated by a pronounced soil, and probably represents a major lake cycle whose age is poorly constrained.

We used statistical approaches to explore the dataset and to better define the mean ages and errors associated with highstands. We removed samples that were from low elevations, from faulted sections, and that represented inverse age-stratigraphy relations. The resulting 47 samples included all data from Coyote subbasin (based on the premise that Lake Manix achieved high levels in order to overflow the threshold to Coyote) and excluded those from Soda Lake. We created a probability distribution using normal kernel density estimates after Lowell (1995) using a procedure developed by G. Balco (Berkeley Geochronology Center; http://cosmognosis.wordpress.com/2011/07/25/what-is-a-camel-diagram-anyway/), which yielded 8 distinct peaks. We then identified the ^{14}C ages contributing to each peak in the distribution, calculated weighted mean ages for these groups, and calibrated each weighted mean using Calib 7.0. The weighted means and errors shown on Fig. 8 agree well with the visually drawn lake-level curve for highstands younger than 41 ka, and they also support two short-lived highstands within P6 as suggested by the outcrop-based thin dashed line. The curve suggests that Lake Manix repeatedly fluctuated over a range of at least 20 m in altitude during MIS 3, from 45 to 25 ka, and that it achieved minimum 541-m highstands in the main part of the basin at least 7 times, 5 of which are corroborated by dated Coyote subbasin deposits. The youngest three highstands, P6–8, all reached 543 masl. Three undated sets of beach deposits at 543 masl are present in Coyote subbasin and may correspond to P6–8.

https://doi.org/10.1016/j.yqres.2014.11.003 Published online by Cambridge University Press

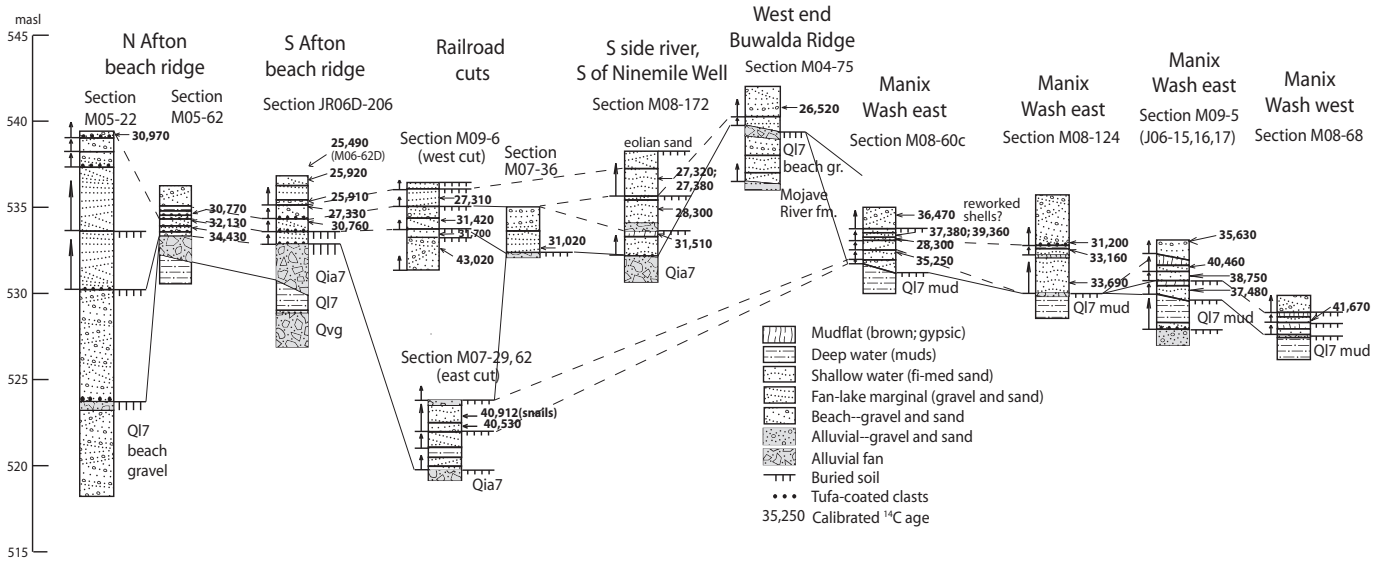

Figure 7. Correlations and altitudes of measured sections from northeast (left) to southwest (right). Solid lines indicate either physically traced contacts or firm contacts with the basal older Qia7 alluvial or Ql7 lacustrine units as mapped by Reheis et al. (2014b). Dashed lines represent correlations on the basis of calibrated ages and soils. See Fig. 2 and Table 1 for additional information.

The lake-level curve is subject to several sources of error. (1) Several ages for the older units > 38 ka are near the practical limit of radiocarbon dating and have relatively large error bars, and a smaller number of ages constrain these units than are available for the younger units. Further, it is possible that the older ^{14}C ages may be minimum values due to contamination or replacement by minute amounts of younger carbonate (Zimmerman et al., 2012), despite analytical efforts to remove surface carbonate using HCl. Thus, the duration and age of the oldest lake cycles (particularly P1, ~44–42 ka, P2, ~40–38.5 ka, and P3, ~37–35.5 ka) are less certain than for younger lake cycles. They may be older than estimated but are unlikely to be younger than the measured ages. However, stratigraphic constraints still apply. The P1 deposits are demonstrably older than P2 deposits based on stratigraphic position and an intervening buried soil; the same applies to P2 and P3. The younger lake phases, P3–P8, are more closely constrained by multiple ages with 2σ error ranges typically less than 300 yr, some of which are replicate ages on the same unit, and by stratigraphy. For example, two ages from site M09-6 (west railroad cut; Figs. 7 and 8) have overlapping error ranges, but are separated in outcrop by a weak buried soil, requiring a hiatus of perhaps several hundred years between the two dated beds.

(2) The Manix basin is traversed by several Quaternary faults (Fig. 2; Miller and Yount, 2002; Miller et al., 2011), and it is possible

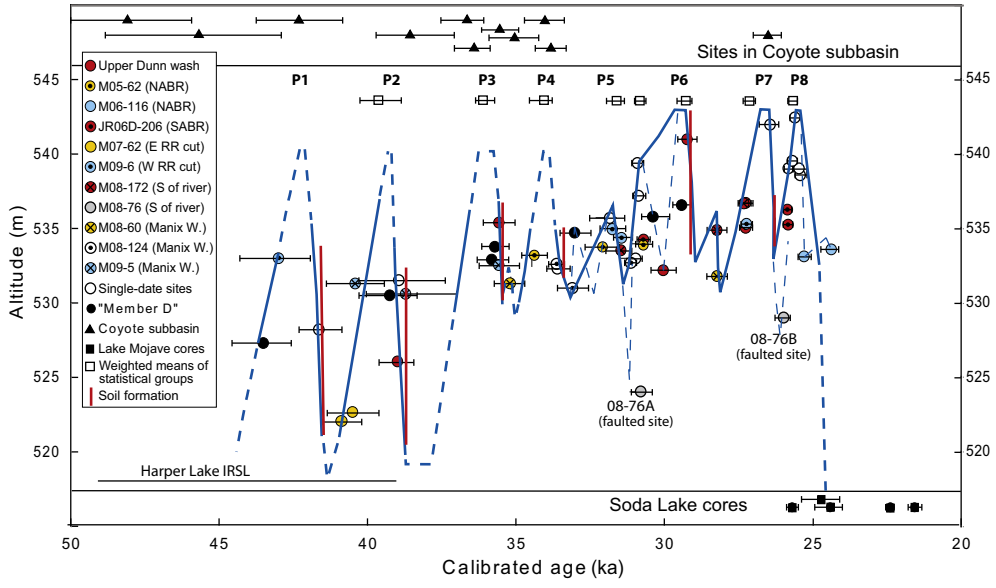

Figure 8. Plot showing calibrated radiocarbon ages with 2σ error bars vs. altitude and reconstructed lake-level change. Sites with multiple ages in measured section are color coded. Three ages from sites M08-60 and M09-5 exhibiting age reversals are omitted (see text for discussion). Ages from Coyote subbasin and Lake Mojave are not plotted by altitude. P1–P8 are numbered highstands of Lake Manix. Boxes with errors below P2–P8 labels are weighted means of age groups as discussed in text. Solid blue lines indicate maximum and minimum lake level defined by tracing dated units; upwardly dashed lines indicate level required to spill over bedrock threshold into Coyote subbasin (Fig. 2) as indicated by dated samples there. Thin dashed lines indicate possible minor lake-level fluctuations either not bounded by soils or constrained by only one date. Bar indicates age range (1σ) of infrared stimulated luminescence dates from Harper Lake sediments (Garcia et al., 2014).

https://doi.org/10.1016/j.yqres.2014.11.003 Published online by Cambridge University Press

that tectonic movement has affected the altitudes of some dated units. The primary active fault in the area of dated deposits is the left-lateral Manix fault. Mapping suggests that late Quaternary displacement on this fault has been significant near Buwalda Ridge and Manix Wash (Reheis et al., 2014b). It is possible that fault-related offset or compression may have slightly altered the altitudes of the sites in this area. A site on the south side of the river, M08-76, lies on the apparently downthrown side of the Manix fault. Thus, the notably lower altitudes of the two ages from this site are questionable (Fig. 8) but the ages are still consistent with lake phases defined at other unfaulted sites.

(3) One source of error that is difficult to assess is the possibility that the Mojave River might have been diverted to the Harper Lake basin upstream at times (Fig. 1). Meek (1999) obtained ^{14}C ages on *Anodonta* from Harper Lake and hypothesized two lake phases, a younger one at around 25 ka (uncalibrated) and an older one that was based on a single infinite age. However, recent work by Garcia et al. (2014) redated the same deposits using luminescence and ^{14}C; they interpreted the results to most likely indicate a single Harper highstand from ~45 to 40 ka. With error bars, however, their accepted luminescence ages span the interval from 49 to 39 ka, which overlaps the P1 and P2 Manix phases (Fig. 8). There are three scenarios that can explain these data: (a) Harper Lake filled prior to both the ~43 and ~40-ka Manix lake phases; (b) Harper Lake filled due to river avulsion between these two phases—if so, this would represent a relatively long pluvial phase; or (c) an energetic Mojave River simultaneously filled both lakes, as hypothesized by Enzel et al. (2003). In any case, Harper Lake could have filled first and then spilled downstream to fill Lake Manix. The large errors on both the Manix ^{14}C and Harper luminescence ages make it impossible to choose among these scenarios.

(4) Another source of error, particularly for older lake phases, is that the Mojave River at times flowed directly into Coyote subbasin, potentially filling it and overflowing southward into the Cady subbasin (Figs. 2 and 8). The river flowed directly into the Coyote subbasin at intervals following the last known full-lake highstand, P8, until as late as ~13(?) cal ka BP (Meek, 1994; Miller et al., 2009), and as described above, did so at least once during MIS 3. Such an episode might have occurred during phase P3 because ages of lake deposits in Coyote subbasin are slightly older than ages assigned to P3 in the main Manix basin (Fig. 8). The Coyote subbasin is smaller than the main Manix basin, so direct filling of Coyote during pluvial phases may have led to discharge into the main basin over the 541-m sill. More complex scenarios are also possible given the available ^{14}C ages. For example, the river could have first filled Coyote at the onset of P3, then the lake could have spilled or the river diverted into the main Manix basin in the later part of P3, then diverted back to directly fill Coyote during which time a soil formed in the basin to the south, and then Coyote could have overflowed once again during P4 to fill all the subbasins. In this case, a pluvial phase might have persisted through P3 and P4, from about 36 to 33 ka. Such a scenario is hinted at by multiple soils close to 35 ka in Coyote subbasin deposits.

Discussion

The level of Lake Manix was controlled largely by precipitation in the San Bernardino Mountains and consequent Mojave River discharge (Reheis et al., 2012). Lake level is a direct record of the balance of precipitation vs. evaporation, in contrast to most other MIS-3 paleoclimate records in the southwestern US that have relied on interpretation of proxies such as stable isotopes, plant macrofossils, pollen, and microfauna. The Manix record does not depend on extrapolation of sedimentation rates between dated strata or correlated paleomagnetic fluctuations, as commonly applied to sediment cores. Within the constraints of the calibrated ^{14}C ages, outcrop preservation, and assumptions regarding interbasin connections, therefore, the Manix deposits should provide one of the most accurate histories of MIS-3 precipitation changes in the southwestern US.

Manix lake level history

The directly dated outcrops recorded at least 8 major lake phases, P1–P8, from about 45 to 25 cal ka BP during MIS 3 and early MIS 2 (Fig. 8) before the threshold at Afton Canyon was incised and Lake Mojave formed downstream. These phases lasted about 1000–1500 yr and were separated by periods of lake-level decline >15–20 m during which weak soils formed on nearshore deposits preserved above lake level. Using the weighted means of dates (Fig. 8), highstands of phases P2–P8 occurred at about 43, 39.7, 36.1, 34.1, 31.6, 30.8, 29.4 (two quick fluctuations in P6), 27.2, and 25.6 ka, respectively; phases P1–P3 have larger age errors and could be older. At some sites, sufficient age control exists to indicate minor lake-level fluctuations within a lake phase, as suggested by the thin dashed lines in Fig. 8. The average time between major highstands is 2.0 kyr with a range of 0.7–3.6 kyr. Such periodicity indicates millennial-scale changes in precipitation delivered to southwestern California and specifically to the Transverse Ranges, as inferred from other lake records in the region (e.g., Phillips et al., 1994; Lin et al., 1998; Benson et al., 2003; Kirby et al., 2006).

Early lake phases P1–3 clearly demonstrate the >20 m maximum lake-level changes. The P1 and P2 phases may have been of relatively long duration, as shown in Fig. 8, but also could have been shorter, similar to the better dated younger phases. If so, the early lowstand durations may have been as long as ~3000 yr. P6 may include two highstands, as also suggested by the statistical analysis, though the younger of the two is supported by only two dates. In fact, one could view P5 and the two possible highstands in P6 as one long relatively wet period punctuated by two lake-level drops that were not long enough for recognizable soils to have formed. A smaller lake phase (unnumbered) at about 29 ka between P6 and P7 is supported by only two ages. The end of phase P8 is not well constrained because the highstand was terminated by incision of the threshold at Afton Canyon (Reheis and Redwine, 2008).

Comparison to southwestern US and global climate records

To assess the regional response to global climate perturbations, the Manix lake-level record can be compared to other, more highly resolved isotopic records within the southwestern US region, including Pacific marine cores, and to the MIS 3 isotopic record from the North Greenland Ice Project (NGRIP) ice core in Greenland (Fig. 9; NGRIP members, 2004a). Two recent MIS 3 records (Asmerom et al., 2010; Wagner et al., 2010) are on well-dated speleothems from caves in Arizona and New Mexico near the same latitude as Lake Manix. Both speleothem records indicate that the southwestern US was relatively cool and wet during the D–O stadials, although there are minor differences in the timing of identified D–O phases of these records, specifically D–O interstadials 6, 5, and 3. Possibly these differences are due to varying influence of the North American monsoon, which strengthens to the east into New Mexico today and likely also did so in the past (Roy et al., 2013; Sionneau et al., 2013). The Manix highstand periods mostly coincide with the cool wet periods recorded in the speleothems. Remarkably, the Manix highstands closely match the D–O stadials recorded in the NGRIP core, and the soils coincide with abrupt transitions to interstadials. Two of the Lake Manix highstands occurred in the intervals just preceding, and appear to have terminated coincident with, Heinrich events H4 and H3 at about 39 and 30 ka. Although P8 was terminated by incision of the Afton Canyon threshold, it forms the end of a long two-stage highstand preceding H2 at about 24.5 ka (Fig. 9; ages of events from Hemming, 2004, as modified by NGRIP record: NGRIP members, 2004a; Marcott et al., 2011). The duration and timing of three closely spaced lake-level rises that are recorded by P5 and P6, anchored by 15 ^{14}C dates, match the duration of the long stadial between D–O interstadials 5 and 4.

Marine cores off the Pacific coast directly west of Lake Manix yielded proxy records of changes in the California Current that are interpreted

https://doi.org/10.1016/j.yqres.2014.11.003 Published online by Cambridge University Press

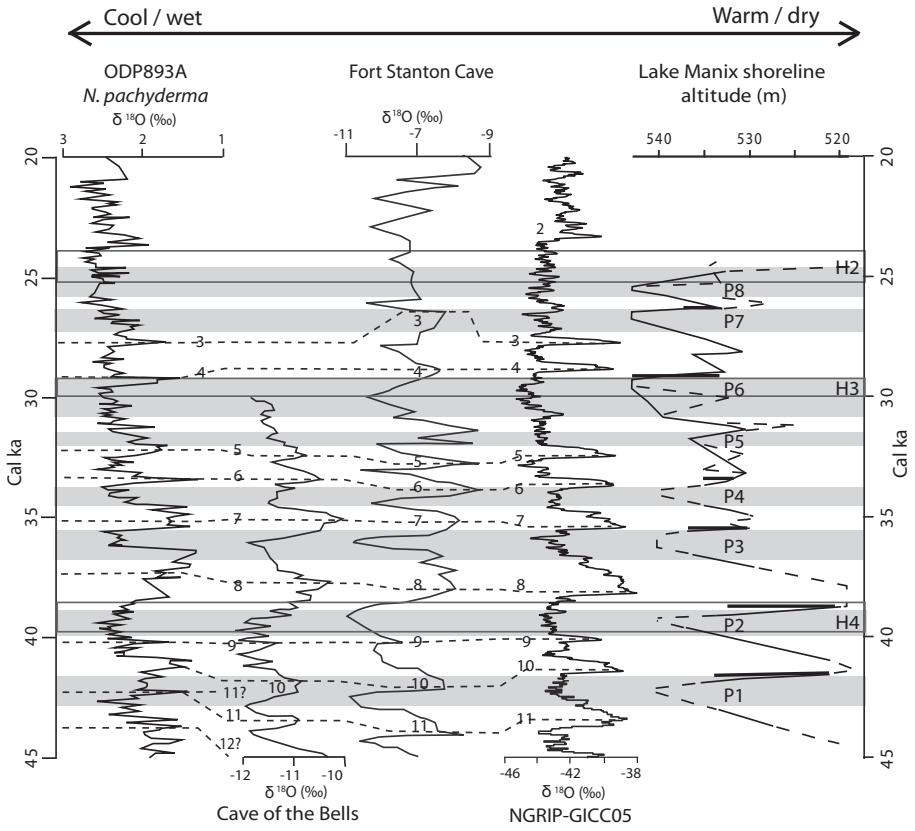

Figure 9. Comparison of marine core ODP893A off the coast of southern California (redrawn from Hendy, 2010; Fig. 1), isotopic records from speleothems in Arizona (redrawn from Wagner et al., 2010) and New Mexico (redrawn from Asmerom et al., 2010), NGRIP ice core (NGRIP members, 2004b; NGRIP Dating Group, 2006), and Manix lake-level curve. Heavy horizontal lines on lake-level curve are soils as shown in Fig. 8. Gray bands represent approximate duration of Manix lake phases P1–P8. Numbers and black dashed lines represent D–O interstadials as identified in publications listed above; queried numbers 11 and 12 show alternative interpretation of Hendy and Kennett (2000). H2–H4 in wide boxes represent intervals of Heinrich events (ages from Hemming, 2004, as modified by dating of NGRIP record: NGRIP members, 2004a; Marcott et al., 2011).

as responses to changes initiated by D–O oscillations in the North Atlantic (e.g., Hendy and Kennett, 2000; Hendy, 2010; Pak et al., 2012). Hendy (2010) used the records from core ODP893A and two other nearby cores to show that foraminifera-based SSTs increased during D–O interstadials. The age models in these cores were based on radiocarbon ages back to 30 ka and linear interpolation by correlation of interstadials, identified by $\delta^{18}O$ data in the marine cores and in the GISP2 ice-core record, beyond 30 ka. Thus, the pre-30-ka records from these cores are tuned to Greenland ice chronology, though the match between these records appears to be poor for interstadials 11 and 12 (Fig. 9). Despite some apparent age offsets, if the suggested correlations to D–O interstadials (Hendy, 2010) are accurate, then most of the periods of higher Manix lake levels corresponded with cooler SSTs.

In general, the yearly change in SST along the southern California coast, driven by expansion in winter and contraction in summer of the Aleutian low relative to the northeast Pacific high, is accompanied by increases in winter–spring precipitation delivered by westerly storms (Hickey, 1979). This annual pattern, amplified in El Niño years, has been invoked as an analog for larger-scale SST changes during stadial (southward shift in Aleutian low) and interstadial (northward shift) conditions (e.g., Hendy and Kennett, 2000; Yamamoto et al., 2007). Other proxy records more closely related to precipitation from the same marine cores indicate that pine forests in southern California expanded downslope during MIS 3 stadials (Heusser, 1998), and that pulses of increased runoff occurred at about 45, 35, 30, and 25 ka (Robert, 2004); all but the oldest of these pulses are coeval with Lake Manix highstands. Together, these speleothem and marine records support a correlation of higher precipitation, or at least greater effective moisture, in the Desert Southwest with D–O stadials.

Comparison to other lake- and water-level records

Well-dated, direct records of lake level and precipitation during MIS 3 that do not rely on interpretation of stable-isotope proxies are scarce in the southwestern deserts. Broad trends in the levels of Lake Babicora in the Chihuahuan Desert of Mexico (Metcalfe et al., 2002), southeast of Lake Manix, and groundwater in Browns Room of Devils Hole (Szabo et al., 1994) to the northeast, are similar, but the level of detail makes comparison with Manix lake level variations difficult (Fig. 10). Both locations show higher water levels prior to ~45 ka (predating the Manix record), from 43–40 ka, overlapping with P2, and generally high levels ~35–25 ka. The Browns Room water levels do not appear to closely correspond with trends in the Devils Hole $\delta^{18}O$ record, which has been interpreted as a proxy for Pacific SST (Winograd et al., 2006). The groundwater table at Valley Wells, northeast of Lake Manix, similarly rose by about 60 ka and remained high until about 20 ka (Pigati et al., 2011). A noble-gas record derived from Mojave River groundwater indicates about 4°C cooler temperature and vigorous aquifer recharge from greater or more intense precipitation from about 43 to 12 ka (Kulongoski et al., 2009). Preliminary results from Las Vegas Valley in southern Nevada suggest that groundwater levels responded to millenial-scale climate changes during MIS 3 (Springer et al., 2013).

A new core from Lake Babicora has yielded a more highly resolved proxy record (Fig. 10) interpreted to indicate that runoff and lake level increased during warm interstadials of MIS 3 due to a stronger influence of the North American summer monsoon, particularly the easterly monsoon sourced from the Gulf of Mexico, and was negatively correlated with westerly winter storms (Roy et al., 2013). The authors

https://doi.org/10.1016/j.yqres.2014.11.003 Published online by Cambridge University Press

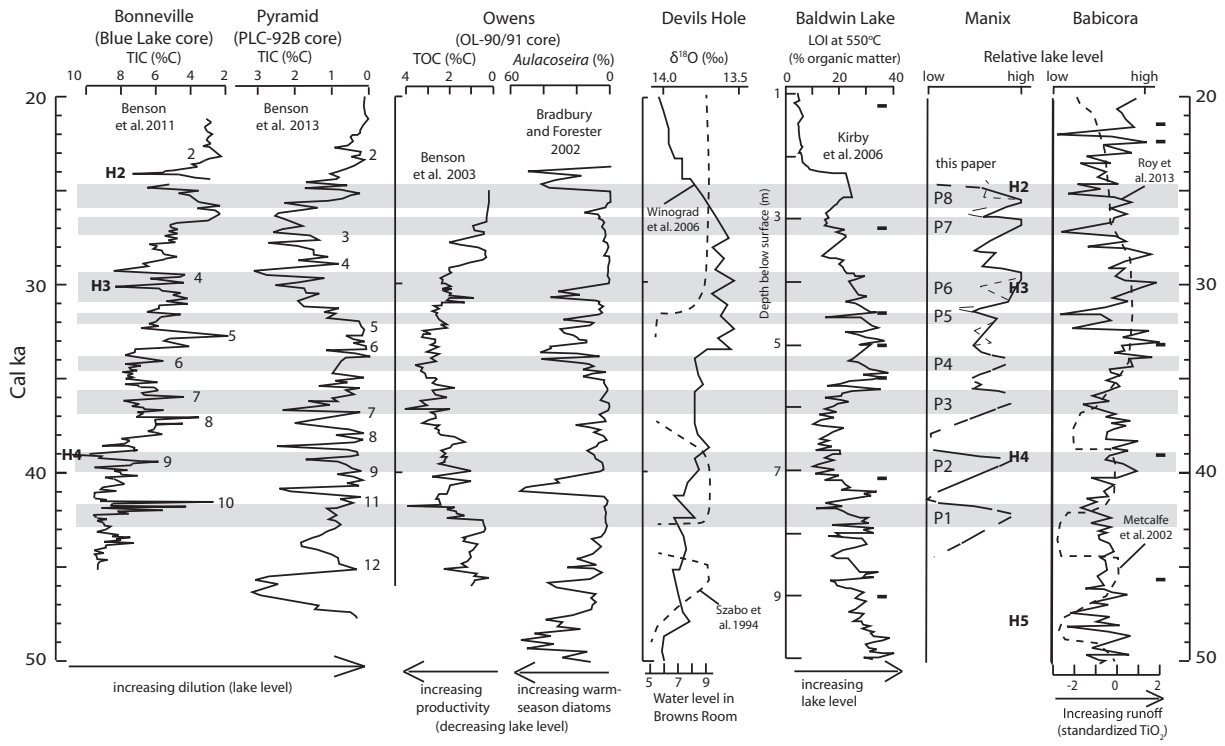

Figure 10. Comparison of Manix lake-level curve with proxy records of Great Basin lakes arranged roughly from north to south. Numbers (D–O interstadials) and H2–H4 (Heinrich events) on Bonneville (Benson et al., 2011) and Pyramid (Benson et al., 2013) records are as shown in cited references; H2–H4 on Manix curve are as shown in Fig. 9. Gray bars are Lake Manix highstands. Thick lines on Baldwin and Babicora plots show positions of ^{14}C dates; note that Baldwin plot is scaled by depth below surface, not time, as in Kirby et al. (2006). All curves except Manix redrawn from source references.

postulate that this enhanced monsoon may have been due to a northward migration of the ITCZ during interstadials. Such conditions are also proposed by Sionneau et al. (2013) based on a core in the Gulf of Mexico. The records from Lakes Babicora and Manix may be at least partly anti-phased due to the lack of monsoon influence in the Manix drainage basin.

Baldwin Lake, in the San Bernardino Mountains near the Mojave River headwaters, is the closest lake record (Fig. 1). A core from this lake is interpreted to indicate alternating ephemeral and permanent lake status (Fig. 10; Kirby et al., 2006). Though ages in the older part of the core are few and are beyond the effective range of radiocarbon dating, Kirby et al. (2006, Fig. 5) note a general correspondence of wetter conditions with higher (warmer) $\delta^{18}O$ values in Greenland ice prior to about 40 ka, and suggest that wetter conditions correspond with D–O interstadials. However, in sediment younger than 40 ka where ^{14}C ages on macrofossils are more reliable, there is little correspondence in the Baldwin Lake and Lake Manix or Greenland records (compare Figs. 9 and 10). We suggest that the limited age control prior to 40 ka could allow this proxy curve to be aligned differently with the GISP2 ice record.

Searles Lake, 150 km northwest of Lake Manix, has a lake-level record based on both outcrop and subsurface stratigraphy (Smith, 2009, and papers cited therein; Lin et al., 1998). This lake filled in response to spillover from the glacially fed Owens Lake upstream, so the Searles record is abrupt—the lake filled when Owens was overflowing and then dried up—and has an uncertain amount of lag time in response to changes in climate. During MIS 3, Searles Lake oscillated from deposition of mud during perennial-lake conditions to deposition of salt during desiccation. Salt layers dated using U–Th techniques were interpreted to indicate seven low-lake levels that were correlated with D–O interstadials recorded in Greenland ice (Phillips et al., 1994; Lin et al., 1998), consistent with our findings for Manix highstands.

Benson et al. (2003) interpreted high total organic carbon (TOC) in Owens Lake (Fig. 10) to reflect increased productivity when glacial flour input decreased during non-glacial periods corresponding to D–O interstadials, and Phillips (2008) correlated the higher TOC intervals to periods of salt deposition representing drier conditions in Searles Lake. In contrast, Benson et al. (2003), by correction of age models originally based on bulk-carbon ^{14}C ages using a series of correlations of magnetic events in cores from Owens, Mono, Pyramid, and Summer Lakes, concluded that all these lakes rose during interstadials of MIS 3. An independent diatom record from Owens Lake (Fig. 10; ages as given in Benson et al., 1996, not adjusted for reservoir effect) shows millennial-scale fluctuations in the concentration of *Aulacoseira* sp., which blooms in fresh water during the summer (Bradbury and Forester, 2002). Increases in these diatoms could record sustained Owens River discharge due to melting of large Sierran snowpacks, or could indicate increased summer storm activity (Bradbury and Forester, 2002). However, there is little correspondence between the two Owens records, either positive or negative, except that both TOC% and *Aulacoseira* abundance are low from about 30 to 25 ka. Several of the Manix highstands occurred during periods of low concentrations of *Aulacoseira* and low productivity, suggesting either cooler periods of low summer rainfall or of low Owens River discharge in the southern Sierra Nevada at these times.

Lake Russell (Pleistocene Mono Lake), farther north, has a well-studied MIS 3 record preserved in outcrops of the Wilson Creek formation (Lajoie, 1968; Benson et al., 2003; Zimmerman et al., 2011). However, there is controversy about the age of this section, which is inferred to extend from 39 to 21 ka by Benson et al. (2003), supported recently by Negrini et al. (2014), and from 65 to 21 ka by Zimmerman et al. (2011) and Vazquez and Lidzbarski (2012). Such a large difference in age range prevents making correlations between Lakes Russell and Manix until this issue is resolved.

Two other core-based high-resolution MIS 3 records (Fig. 10) exist for Pyramid Lake, part of Lake Lahontan (Benson et al., 2013), and for Lake Bonneville (Benson et al., 2011); these lakes lie far north of Lake Manix. Lake level is interpreted to vary inversely with total inorganic

https://doi.org/10.1016/j.yqres.2014.11.003 Published online by Cambridge University Press

carbon content (TIC), which should become less concentrated as lake water freshens. Benson et al. (2011, 2013) correlate these fresher intervals during MIS 3 with increased runoff during D–O interstadials. We note, however, that several of the fresher intervals do not correspond with numbered interstadials, and the age models suggest mismatches between the two records.

In summary, generally high Manix levels through much of MIS 3 are consistent with trends in water tables in nearby locations (Szabo et al., 1994; Quade et al., 1995; Kulongoski et al., 2009; Pigati et al., 2011), with the Searles Lake record (Phillips et al., 1994; Lin et al., 1998) and perhaps with some parts of the Lake Babicora record (Metcalfe et al., 2002; Roy et al., 2013). The Manix record is very similar to those from speleothems in the southern Great Basin, and is supported by recent work on a speleothem in the western Sierra Nevada that recorded wetter conditions during earlier D–O stadials (Oster et al., 2014), but does not appear to match the proxy-based core records from Lake Baldwin to the west (Kirby et al., 2006) and lakes farther north in the Great Basin, including Owens, Lahontan, and Bonneville. There are likely several reasons for these differences among lake records, including their physical setting, latitudinal differences in atmospheric circulation patterns, and problems with radiocarbon dating, core age models, and interpretation of proxies.

Physical setting

Lake Manix was fed directly by one river draining a single source area, the minimally glaciated San Bernardino Mountains (Owen et al., 2003). In contrast, most of the pluvial lakes farther north were at times influenced by glacially mediated runoff from several drainage basins. Lakes Bonneville and Lahontan were also far larger and perhaps not as sensitive as Manix to abrupt climate change. Owens and Pyramid Lakes were mediated by overflow to other basins, and therefore may record timing of lake-level change but not hydrologic maxima. In addition, all the northern lakes discussed above, except for Searles, lie at much higher altitudes than Lake Manix, and therefore are not so strongly controlled by and sensitive to evaporation (Reheis et al., 2012).

Latitudinal position and relations to atmospheric circulation

Benson et al. (1998, 2003, 2011, 2013) and Kirby et al. (2006) inferred that lakes as far north as Chewaucan in southern Oregon and as far south as Baldwin in southern California rose during D–O interstadials in response to a northward shift in the polar jet, controlled by retreat of the Laurentide ice sheet. It is counterintuitive that lakes spanning 8° latitude should behave synchronously during such a northward shift; other papers have concluded that Searles Lake, in the southern Basin and Range, rose during MIS 3 stadials (Phillips et al., 1994; Lin et al., 1998). Pluvial lakes are known to have reached highstands during MIS 2 at times that varied with latitude (Thompson et al., 1993; Bartlein et al., 1998). More recently, Lyle et al. (2012) proposed that Great Basin lakes did not reach MIS 2 highstands that followed a north–south migration of westerlies, but rather that high lake levels migrated from southeast to northwest following shifting precipitation patterns driven by incursion of tropical moisture from the Gulf of Mexico and the eastern Pacific. Such an interpretation is consistent with older MIS 2 highstands in the southernmost lakes (Mojave—Wells et al., 2003; Babicora—Metcalfe et al., 2002; Estancia—Allen and Anderson, 2000) and, by analogy, suggests that MIS 3 lake level change would not have been synchronous throughout the Great Basin.

Radiocarbon dating and age models

Lake-level records derived from study of outcrops can be directly dated but rely on accurate correlations and intensive field work and usually yield only a medium-resolution record (several hundreds to a few thousand years). In contrast, core studies commonly rely on construction of age models from ^{14}C ages and occasionally, other markers such as tephra layers of known age (e.g., Benson et al., 2003). Both approaches must contend with potentially large and time-variable errors in reservoir effects of old carbon, increasing effects of contamination by young carbon in older samples, and analytical and calibration errors that increase with sample age, particularly in samples older than ~30 ka. We attempted to minimize these errors by applying a reservoir correction measured on paired charcoal and shells of Holocene age and by obtaining multiple ages on several stratigraphic sequences of the same age, thus allowing calculation of weighted averages. These efforts reduced the 2σ error ranges to less than about 400 yr for the younger lake cycles P6–8, but larger errors of ~600 yr for P5 to 1200 yr for P2 (Fig. 8).

Recently, efforts have been made to refine age models of cores from Great Basin lakes by measuring paleomagnetic secular variation (PSV) in core sediments to correlate PSV patterns between lakes and thence to those of North Atlantic marine cores (Benson et al., 2011, 2013) that in turn are dated by matching, or tuning, to the $\delta^{18}O$ variations in the marine and Greenland GISP2 cores. PSV has promise for correlation of lake records around the Great Basin, but thus far lacks a reference curve with a good density of reliable ages such as well-dated tephra layers and macrofossils (S. Zimmerman, Lawrence Livermore National Lab., written commun. 2014). Although such tuning has become an accepted practice in marine- and ice-based paleoclimate studies, particularly in the North Atlantic, Austin and Hibbert (2012, p. 28) warned that "the phasing of climatic events between the different palaeoclimatic 'archives' cannot be assessed" if such archives are tuned assuming that the changes are synchronous. Blaauw (2012) further noted that inherent variability combined with measurement error can allow asynchronous events in different proxy records to be interpreted as synchronous and that the GISP2 and NGRIP timescales differ beyond 40 ka; he recommended that individual proxy records be kept on independent timescales.

A further complication arises from the newly revised IntCal13 dataset, based on much improved chronologies (Reimer et al., 2013). This revision, when applied to the Manix radiocarbon dates in the range of ~26–35 ka, resulted in shifts of up to 700 yr younger compared to dates calibrated using IntCal09 (Reimer et al., 2009). It is possible that recalibration of radiocarbon dates from some cores may result in different correlations of lake proxies to marine and ice records. We note these issues to illustrate the difficulties in obtaining, dating, and interpreting high-resolution records from cores and in correlating them to other climate records, especially when such records are widely separated geographically.

Core proxies

Outcrops directly record lake level change (reviewed in Reheis et al., 2014a), whereas core studies mainly infer lake level from interpretation of proxies such as stable isotopes that may be influenced by several competing factors whose relative effects may be difficult to assess. Both the Bonneville and Pyramid cores were tuned to marine core PSV and in turn to GISP2 (Benson et al., 2011, 2013); yet the two cores do not show obvious synchronous behavior in their proxy records (Fig. 10), and correlations with D–O interstadials in some cases seem somewhat arbitrary. Are these differences the result of different behavior of inorganic carbon in the two lake basins and (or) relatively small errors in age models, or are they real reflections of leads and lags in response to climate change?

Implications for atmospheric controls on lake level

Our study demonstrates that Lake Manix experienced significant fluctuations in lake level during MIS 3. With the constraints on ^{14}C dating, we are confident that after ~33 ka, the lake rose during Greenland stadials (NGRIP members, 2004a), and fell during interstadials. By extension, and given the close match between the Lake Manix and NGRIP records, it seems likely that the older highstands also occurred during stadials. This lake-level record corresponds well with cool wet intervals dated by uranium-series techniques in speleothems from

https://doi.org/10.1016/j.yqres.2014.11.003 Published online by Cambridge University Press

caves at similar southern latitudes (Asmerom et al., 2010; Wagner et al., 2010) and with pollen studies from core ODP893A (Heusser, 1998; Hendy and Kennett, 2000) (Fig. 9). However, the timing of Manix highstands and the southern speleothem records is opposite to that inferred from proxy records in sediment cores and sections for lakes farther north (Fig. 10), ranging across 6° of latitude (Zic et al., 2002; Benson et al., 2003, 2011, 2013). If all the chronologies are correct, and this is by no means certain, this implies an air-mass boundary that, during pluvial periods at Lake Manix, lay at about 36°N as suggested by Garcia et al. (2014), blocking moisture from lakes that lay farther north, and during interpluvials, migrating far enough north to fill lakes between 36° and 43°N simultaneously but reducing moisture to Lake Manix. We suspect Laurentide ice extent or height would not have fluctuated dramatically enough during MIS 3 at periodicities of only 1–3 kyr to have had such a large effect on lake level. So what could control such a boundary?

Various studies have proposed alternative hypotheses for abrupt changes in climate in the Pacific Ocean and adjacent continental areas during MIS 3 as a result of teleconnections to North Atlantic D–O events, including ENSO-like variability (Clement, 1999; Merkel et al., 2010), north–south movements of the ITCZ (Yamamoto et al., 2007; Leduc et al., 2009), changes in insolation (Robert, 2004; Kirby et al., 2006; Hendy, 2010), and precessional forcing (Robert, 2004; Yamamoto et al., 2007). Most of these hypotheses envision a weakening of the North Pacific high and strengthening of the Aleutian low during stadials in response to external forcing. Most studies (except Robert, 2004) discuss the effects of such changes on SST and coastal currents and not on precipitation, except indirectly (e.g., El Niño-like conditions should increase rainfall in coastal California). Lyle et al. (2012) proposed that during MIS 2, northeasterly flow of moisture from the tropical Pacific was responsible for high lake levels due to the steep SST gradient present along the California coast.

SST gradients also play a role in another important climate cycle in the Pacific Ocean, the North Pacific Gyre Oscillation (NPGO; Di Lorenzo et al., 2008). During a negative NPGO index, the polar jet becomes more meridional and its average position is shifted to the south, causing an increase in storm frequency in southern California (e.g., Hurrell, 1995; Livezey et al., 1997; Chang et al., 2002; McAfee and Russell, 2008; Kulongoski et al., 2009). Reheis et al. (2012) found that a fresh to moderately saline lake persisted in the Manix basin for much of the past 500 ka, including parts of interglacials MIS 5, 7, and 9. They interpreted this to indicate that atmospheric or ocean circulation patterns, rather than the position of ice sheets, controlled the influx of moisture to the southwestern US, and proposed that the cause may have been steep SST gradients analogous to those that increase the frequency of atmospheric river-type storms (e.g., Neiman et al., 2004; Ralph et al., 2004; Dettinger et al., 2011; Rutz and Steenburgh, 2012) along the California coast. These storms deliver large amounts of moisture sourced from the tropical Pacific (Mo and Higgins, 1998; Jones, 2000). Reheis et al. (2012) showed a strong correlation between atmospheric-river storms, historic Mojave River discharge, and the negative phase of NPGO. Rutz and Steenburgh (2012) showed that the impact of such storms today extends eastward from the California coast to central New Mexico. We suggest that precipitation in southern California, and perhaps to a lesser extent Arizona and New Mexico, during MIS 3 may have been enhanced during stadials by an increased frequency of storms entraining tropical moisture in response to a steepening of the SST gradient. Additional evidence for at least episodic incursions of warm tropical moisture comes from the common presence, in late Pleistocene and older Lake Manix sediments (Steinmetz, 1987; Reheis et al., 2012) of *Limnocythere bradburyi*, an ostracode that today lives only south of the Mexican border in lakes supported mainly by summer rainfall (Forester, 1985). Expansion of the Aleutian low in response to stadial events in the North Atlantic, as suggested by models (Okumura et al., 2009), should cause such steepening and increased storm frequency, as occurs today in negative NPGO conditions (Zhang and Delworth, 2007).

Would increases in precipitation during MIS 3 stadials have extended farther north into the Great Basin? Previously published core studies from lakes north of 36° suggest just the opposite (Zic et al., 2002; Benson et al., 2003, 2011, 2013). Assuming the age models and isotopic interpretations in these studies are correct, perhaps the antiphased behavior records more northward penetration of moisture as the Aleutian low shrank during interstadials. However, as pointed out by Lyle et al. (2012), such behavior during MIS 2 and the deglaciation is not supported by the temporal pattern of high lake levels in the Great Basin and wet conditions on the coast. Instead, they suggested a northwestward progression toward wetter conditions through time. Whether such a temporal progression occurred during stadial-interstadial fluctuations of MIS 3 cannot be addressed without more independently dated high-resolution records.

Conclusions

Stratigraphic studies and radiocarbon dates on nearshore deposits of Lake Manix show that lake level fluctuated repeatedly over a range of 10–20 m during MIS 3, from about 45 to 25 ka. At least eight highstands occurred during this time; we are confident that the youngest four, P5–P8, correspond with the timing of Greenland stadials in the NGRIP record. The highstands indicate much higher Mojave River discharge and, thus, periods of increased precipitation in the San Bernardino Mountains. Their timing is consistent with wet cool periods recorded in cave speleothems from southern Arizona and New Mexico (Asmerom et al., 2010; Wagner et al., 2010), and also with pollen records of higher rainfall on the southern California coast (Heusser, 1998; Lyle et al., 2012). Our study pushes the boundary of detectable millennial-scale changes that can be correlated to the Greenland ice core record, due to limitations inherent in radiocarbon dating and calibration. Nevertheless, we believe that stadial periods in the southern Great Basin and Mojave Desert were cool and wet, in contrast to results for pluvial lakes farther north (e.g., Benson et al., 2003, 2011, 2013). High lake levels in such a low-latitude desert setting as the Manix basin require significant rearrangements of atmospheric circulation and suggest that the southern lakes were sustained by greatly increased precipitation from tropical sources.

Acknowledgments

This study was funded by the U.S. Geological Survey (USGS) Climate and Land Use Research and Development Program. We thank the many field assistants who helped during this study. Gary Skipp (USGS) provided XRD analysis of selected *Anodonta* shell samples, including a modern *A. californiensis* shell contributed by Allan K. Smith of Hillsboro, OR. Andy Cyr (USGS) kindly performed the statistical analysis of ^{14}C ages. Many discussions with George Jefferson (Anza-Borrego Desert State Park, Calif.) and Norman Meek (Calif. State Univ.—San Bernardino) helped our understanding of the Manix history and enabled us to clarify many aspects of their careful work. Finally, we thank Jeff Pigati (USGS), Susan Zimmerman (LLNL), and Rob Negrini (CSUB), whose thorough and helpful reviews greatly improved this manuscript.

References

Allen, B.D., Anderson, R.Y., 2000. A continuous, high-resolution record of late Pleistocene climate variability from the Estancia basin, New Mexico. Geological Society of America Bulletin 112, 1444–1458.

Antevs, E., 1948. Climatic changes and pre-white man in the Great Basin, with emphasis on glacial and post glacial times. Bulletin of the University of Utah 38, 168–191.

Asmerom, Y., Polyak, V.J., Burns, S.J., 2010. Variable winter moisture in the southwestern United States linked to rapid glacial climate shifts. Nature Geoscience 3, 114–117.

Austin, W.E.N., Hibbert, F.D., 2012. Tracing time in the ocean: a brief review of chronological constraints (60–8 kyr) on North Atlantic marine event-based stratigraphies. Quaternary Science Reviews 36, 28–37.

Bacon, S.N., Burke, R.M., Pezzopane, S.K., Jayko, A.S., 2006. Last glacial maximum and Holocene lake levels of Owens Lake, eastern California, USA. Quaternary Science Reviews 25, 1264–1282.

Bartlein, P.J., Anderson, K.H., Anderson, P.M., Edwards, M.E., Mock, C.J., Thompson, R.S., Webb, R.S., Webb, T.I.I.I., Whitlock, C., 1998. Paleoclimate simultations for North America over the past 21,000 years: features of the simulated climate and comparisons with paleoenvironmental data. Quaternary Science Reviews 17, 549–585.

Benson, L., Kashgarian, M., Rubin, M., 1995. Carbonate deposition, Pyramid Lake subbasin, Nevada: 2. Lake levels and polar jet stream positions reconstructed from radiocarbon ages and elevations of carbonates (tufas) deposited in the Lahontan basin. Palaeogeography, Palaeoclimatology, Palaeoecology 117, 1–30.

Benson, L.V., Burdett, J.W., Kashgarian, M., Lund, S.P., Phillips, F.M., Rye, R.O., 1996. Climatic and hydrologic oscillations in the Owens Lake basin and the adjacent Sierra Nevada, California. Science 274, 746–749.

Benson, L.V., Lund, S.P., Burdett, J.W., Kashgarian, M., Rose, T.P., Smoot, J.P., Schwartz, M., 1998. Correlation of late-Pleistocene lake-level oscillations in Mono Lake, California, with North Atlantic climate events. Quaternary Research 49, 1–10.

Benson, L., Lund, S., Negrini, R.M., Linsley, B., Zic, M., 2003. Response of North American Great Basin lakes to Dansgaard–Oeschger oscillations. Quaternary Science Reviews 22, 2239–2251.

Benson, L.V., Lund, S.P., Smoot, J.P., Rhode, D.E., Spencer, R.J., Verosub, K.L., Louderback, L.A., Johnson, C.A., Rye, R.O., Negrini, R.M., 2011. The rise and fall of Lake Bonneville between 45 and 10.5 ka. Quaternary International 235, 57–69.

Benson, L.V., Smoot, J.P., Lund, S.P., Mensing, S.A., Foit Jr., F.F., Rye, R.O., 2013. Insights from a synthesis of old and new climate-proxy data from the Pyramid and Winnemucca lake basins for the period 48 to 11.5 cal ka. Quaternary International 310, 62–82.

Blaauw, M., 2012. Out of tune: the dangers of aligning proxy archives. Quaternary Science Reviews 36, 38–49.

Blaney, F.H., 1957. Evaporation study at Silver Lake in the Mojave Desert, California. Eos 38, 209–215.

Borbas, J.E., Wheeler, A.P., Sikes, C.S., 1991. Molluscan shell matrix phosphoproteins: correlation of degree of phosphorylation to shell mineral microstructure and to in vitro regulation of mineralization. The Journal of Experimental Zoology 258, 1–13.

Bradbury, J.P., Forester, R.M., 2002. Environment and paleolimnology of Owens Lake, California: a record of climate and hydrology for the last 50,000 years. In: Hershler, R., Madsen, D.B., Currey, D.R. (Eds.), Great Basin Aquatic Systems History, Smithsonian Contributions to the Earth Sciences. Smithsonian Institution Press, Washington, D.C., pp. 145–173.

Chang, E.K.M., Lee, S., Swanson, K.L., 2002. Storm track dynamics. Journal of Climatology 15, 2163–2183.

Clement, A.C., 1999. Orbital controls on the El Niño / Southern Oscillation and the tropical climate. Paleoceanography 14, 441–456.

Cohen, A.S., 2003. Paleolimnology, the History and Evolution of Lake Systems. Oxford University Press, New York.

Cox, B.F., Hillhouse, J.W., Owen, L.A., 2003. Pliocene and Pleistocene evolution of the Mojave River, and associated tectonic development of the Transverse Ranges and Mojave Desert, based on borehole stratigraphy studies and mapping of landforms and sediments near Victorville, California. In: Enzel, Y., Wells, S.G., Lancaster, N. (Eds.), Paleoenvironments and Paleohydrology of the Mojave and Southern Great Basin Deserts. Geological Society of America Special Paper 368, Boulder, Colorado, pp. 1–42.

Denton, G.H., Alley, R.B., Comer, G.C., Broecker, W.S., 2005. The role of seasonality in abrupt climate change. Quaternary Science Reviews 24, 1159–1182.

Dettinger, M.D., Ralph, F.M., Das, Tapash, Neiman, P.J., Cayan, D.R., 2011. Atmospheric rivers, floods and the water resources of California. Water 3, 445–478.

Di Lorenzo, E., Schneider, N., Cobb, K.M., Franks, P.J.S., Chhak, K., Miller, A.J., McWilliams, J.C., Bograd, S.J., Arango, H., Curchitser, E., Powell, T.M., 2008. North Pacific Gyre Oscillation links ocean climate and ecosystem change. Geophysical Research Letters 35, L08607. http://dx.doi.org/10.1029/2007GL032838.

Enzel, Y., 1992. Flood frequency of the Mojave River and formation of late Holocene playa lakes, southern California, USA. The Holocene 2, 11–18.

Enzel, Y., Wells, S.G., 1997. Extracting Holocene paleohydrology and paleoclimatology information from modern extreme flood events: an example from southern California. Geomorphology 19, 203–226.

Enzel, Y., Cayan, D.R., Anderson, R.Y., Wells, S.G., 1989. Atmospheric circulation during Holocene lake stands in the Mojave Desert: evidence of regional climatic change. Nature 44–47.

Enzel, Y., Wells, S.G., Lancaster, N., 2003. Late Pleistocene lakes along the Mojave River, southeast California. In: Enzel, Y., Wells, S.G., Lancaster, N. (Eds.), Paleoenvironments and Paleohydrology of the Mojave and Southern Great Basin Deserts. Geological Society of America Special Paper 368, Boulder, Colo., pp. 61–77.

Forester, R.M., 1985. Limnocythere bradburyi n. sp. a modern ostracode from central Mexico and a possible Quaternary paleoclimate indicator. Journal of Paleontology 59, 8–20.

Garcia, A.L., Knott, J.R., Bright, J., Mahan, S.A., 2014. Geochronology and paleoenvironment of pluvial Harper Lake, Mojave Desert, California. Quaternary Research 81, 305–317.

Hemming, S.R., 2004. Heinrich events: massive late Pleistocene detritus layers of the North Atlantic and their global climate imprint. Reviews of Geophysics 42, RG1005. http://dx.doi.org/10.1029/2003RG000128.

Hendy, I.L., 2010. The paleoclimatic response of the Southern Californian Margin to the rapid climate change of the last 60 ka: a regional overview. Quaternary International 215, 62–73.

Hendy, I.L., Kennett, J.P., 2000. Dansgaard–Oeschger cycles and the California Current System: planktonic foraminiferal response to climate change in Santa Barbara Basin, Ocean Drilling Program hole 893A. Paleoceanography 15, 30–42.

Hereford, R., Webb, R.H., Longpre, C.I., 2006. Precipitation history and ecosystem response to multidecadal precipitation variability in the Mojave Desert region, 1893–2001. Journal of Arid Environments 67, 13–34.

Heusser, L., 1998. Direct correlation of millenial-scale changes in western North American vegetation and climate with changes in the California Current system over the past ~60 kyr. Paleoceanograhy 13, 252–262.

Hickey, B.M., 1979. The California Current system—hypotheses and facts. Progress in Oceanography 8, 191–279.

Hostetler, S., Benson, L.V., 1990. Paleoclimatic implications of the high stand of Lake Lahontan derived from models of evaporation and lake level. Climate Dynamics 4, 207–217.

Hurrell, J.W., 1995. Decadal trends in the North Atlantic Oscillation: regional temperatures and precipitation. Science 269, 676–679.

Ingram, W.M., 1948. The larger freshwater clams of California, Oregon and Washington. Journal of Entomology and Zoology 40, 72–92.

Jefferson, G.T., 2003. Stratigraphy and paleontology of the middle to late Pleistocene Manix Formation, and paleoenvironments of the central Mojave River, southern California. In: Enzel, Y., Wells, S.G. (Eds.), Paleoenvironments and Paleohydrology of the Mojave and Southern Great Basin Deserts. Geological Society of America Special Paper 368, Boulder, Colo., pp. 43–60.

Jones, C., 2000. Occurrence of extreme precipitation events in California and relationships with the Madden–Julian Oscillation. Journal of Climatology 13, 3576–3587.

Kirby, M.E., Lund, S.P., Bird, B.W., 2006. Mid-Wisconsin sediment record from Baldwin Lake reveals hemispheric climate dynamics (Southern CA, USA). Palaeogeography, Palaeoclimatology, Palaeoecology 24, 267–283.

Kirby, M.E., Zimmerman, S.R.H., Patterson, W.P., Rivera, J.J., 2012. A 9170-year record of decadal-to-multi-centennial scale pluvial episodes from the coastal Southwest United States: a role for atmospheric rivers? Quaternary Science Reviews 46, 57–65.

Kulongoski, J.T., Hilton, D.R., Izbicki, J.A., Belitz, K., 2009. Evidence for prolonged El Niño-like conditions in the Pacific during the Late Pleistocene: a 43 ka noble gas record from California groundwaters. Quaternary Science Reviews 28, 2465–2473.

Lajoie, K.R., 1968. Late Quaternary Stratigraphic and Geologic History of Mono Basin, Eastern California. University of California at Berkeley (Ph.D. thesis, 271 pp.).

Leduc, G., Vidal, L., Tachikawa, K., Bard, E., 2009. ITCZ rather than ENSO signature for abrupt climate changes across the tropical Pacific? Quaternary Research 72, 123–131.

Lin, J.C., Broecker, W.S., Hemming, S.R., Hajdas, I., Anderson, R.F., Smith, G.I., Kelley, M., Bonani, G., 1998. A reassessment of U–Th and ^{14}C ages for late-glacial high-frequency hydrological events at Searles Lake, California. Quaternary Research 49, 11–23.

Livezey, R.E., Masutani, M., Leetmaa, A., Rui, H., Ji, M., Kumar, A., 1997. Teleconnective response of the Pacific–North American region atmosphere to large central equatorial Pacific SST anomalies. Journal of Climate 10, 1787–1820.

Lopes-Lima, M., Rocha, A., Goncalves, F., Andrade, J., Machado, J., 2010. Microstructural characterization of inner shell layers in the freshwater bivalve *Anodonta cygnea*. Journal of Shellfish Research 29, 969–973.

Lowell, T.V., 1995. The application of radiocarbon age estimates to the dating of glacial sequences: an example from the Miami Sublobe, Ohio, USA. Quaternary Science Reviews 14, 85–99.

Lyle, M., Heusser, L., Ravelo, C., Yamamoto, M., Barron, J., Diffenbaugh, N.S., Herbert, T., Andreasen, D., 2012. Out of the Tropics: the Pacific, Great Basin lakes, and late Pleistocene water cycle in the western United States. Science 337, 1629–1633.

Marcott, S.A., Clark, P.U., Padman, L., Klinkhammer, G.P., Springer, S.R., Liu, Z., Otto-Bliesner, B.L., Carlson, A.E., Ungerer, A., Padman, J., He, F., Cheng, J., Schmittner, A., 2011. Ice-shelf collapse from subsurface warming as a trigger for Heinrich events. Proceedings of the National Academy of Sciences 108, 13,415–13,419.

McAfee, S.A., Russell, J.L., 2008. Northern Annular Mode impact on spring climate in the western United States. Geophysical Research Letters 35, L17701. http://dx.doi.org/10.1029/2008GL034828.

Meek, N., 1990. Late Quaternary Geochronology and Geomorphology of the Manix Basin, San Bernardino County, California, Department of Geography. University of California, Los Angeles (Ph.D. thesis, 212 pp.).

Meek, N., 1994. The stratigraphy and geomorphology of Coyote basin. In: Reynolds, J. (Ed.), Calico, Coyote Basin & Lake Havasu Giants. San Bernardino County Museum Association Quarterly, pp. 5–13.

Meek, N., 1999. New discoveries about the Late Wisconsinan history of the Mojave River system. In: Reynolds, R.E., Reynolds, J. (Eds.), Tracks Along the Mojave: A Field Guide from Cajon Pass to the Calico Mountains and Coyote Lake. San Bernardino Museum Quarterly, pp. 113–117.

Menking, K.M., Anderson, R.Y., Shafike, N.G., Syed, K.H., Allen, B.D., 2004. Wetter or colder during the Last Glacial Maximum? Revisiting the pluvial lake question in southwestern North America. Quaternary Research 62, 280–288.

Merkel, U., Prange, M., Schulz, M., 2010. ENSO variability and teleconnections during glacial climates. Quaternary Science Reviews 29, 86–100.

Metcalfe, S., Say, A., Black, S., McCulloch, R., O'Hara, S., 2002. Wet conditions during the last glaciation in the Chihuahuan Desert, Alta Babicora basin, Mexico. Quaternary Research 57, 91–101.

Miller, D.M., Yount, J.L., 2002. Late Cenozoic tectonic evolution of the north-central Mojave Desert inferred from fault history and physiographic evolution of the Fort Irwin area, California. Geological Society of America Memoir 195, 173–197.

Miller, D.M., Dudash, S.L., McGeehin, J.P., 2009. Chronology of pluvial Lake Coyote, California, and implications for 25 to 10-ka Mojave River paleohydrology. PACLIM 2009 Abstracts.

Miller, D.M., Schmidt, K.M., Mahan, S.A., McGeehin, J.P., Owen, L.A., Barron, J.A., Lehmkuhl, F., Lohren, R., 2010. Holocene landscape response to seasonality of storms in the Mojave Desert. Quaternary International 215, 45–61.

Miller, D.M., Reheis, M.C., Wan, E., Wahl, D.B., Olson, H., 2011. Pliocene and early Pleistocene paleogeography of the Coyote Lake and Alvord Mountain area, Mojave Desert, California. In: Reynolds, R.E. (Ed.), The Incredible Shrinking Pliocene, pp. 53–67.

https://doi.org/10.1016/j.yqres.2014.11.003 Published online by Cambridge University Press

Mo, K.C., Higgins, R.W., 1998. Tropical convection and precipitation regimes in the western United States. Journal of Climatology 11, 2404–2423.
Muessig, S., White, G.N., Byers Jr., F.M., 1957. Core logs from Soda Lake, San Bernardino County, California. U.S. Geological Survey Bulletin 1045-C, 81–96.
Negrini, R.M., McCuan, D.T., Horton, R.A., Lopez, J.D., Cassata, W.S., Channell, J.E.T., Verosub, K.L., Knott, J.R., Coe, R.S., Liddicoat, J.C., Lund, S.P., Benson, L.V., Sarna-Wojcicki, A.M., 2014. Nongeocentric axial dipole field behavior during the Mono Lake excursion. Journal of Geophysical Research, Solid Earth 119. http://dx.doi.org/10.1002/2013JB010846.
Neiman, P.J., Persson, P.O.G., Ralph, F.M., Jorgensen, D.P., White, A.B., Kingsmill, D.E., 2004. Modification of fronts and precipitation by coastal blocking during an intense landfalling winter storm in southern California: observations during CALJET. Monthly Weather Review 132, 242–273.
NGRIP Dating Group, 2006. Greenland ice core chronology 2005 (GICC05), IGBP PGES / World Data Center for Paleoclimatology. NOAA/NCDC Paleoclimatology Program, Boulder.
NGRIP Members, 2004a. High-resolution record of Northern Hemisphere climate extending into the last interglacial period. Nature 431, 147–151.
NGRIP Members, 2004b. North Greenland Ice Core Project oxygen isotope data, IGBP PAGES / World Data Center for Paleoclimatology. NOAA/NGDC Paleoclimatology Program, Boulder.
Okumura, Y.M., Deser, C., Hu, A., Timmermann, A., Xie, S.-P., 2009. North Pacific climate response to freshwater forcing in the subarctic North Atlantic: oceanic and atmospheric pathways. Journal of Climate 22, 1424–1445.
Oster, J.L., Montanez, I.P., Mertz-Kraus, R., Sharp, W.D., Stock, G.M., Spero, H.J., Tinsley, J., Zachos, J.C., 2014. Millenial-scale variations in western Sierra Nevada precipitation during the last glacial cycle MIS 4/3 transition. Quaternary Research 82, 236–248.
Oviatt, C.G., 1997. Lake Bonneville fluctuations and global climate change. Geology 25, 155–158.
Oviatt, C.G., Thompson, R.S., Kaufman, D.S., Bright, J., Forester, R.M., 1999. Reinterpretation of the Burmester Core, Bonneville Basin, Utah. Quaternary Research 52, 180–184.
Owen, L.A., Finkel, R.C., Minnich, R.A., Perez, A.E., 2003. Extreme southwestern margin of late Quaternary glaciation in North America: timing and controls. Geology 31, 729–732.
Pak, D.K., Lea, D.W., Kennett, J.P., 2012. Millennial scale changes in sea surface temperature and ocean circulation in the northeast Pacific, 10–60 ka. Paleoceanograhy 27, 13.
Phillips, F.M., 2008. Geological and hydrological history of the paleo-Owens River drainage since the late Miocene. In: Reheis, M.C., Hershler, R., Miller, D.M. (Eds.), Late Cenozoic Drainage History of the Southwestern Great Basin and Lower Colorado River Region: Geologic and Biotic Perspectives. Geological Society of America Special Paper 439, Boulder, Colorado, pp. 115–150.
Phillips, F.M., Campbell, A.R., Smith, G.I., Bischoff, J.L., 1994. Interstadial climate cycles: a link between western North America and Greenland? Geology 22, 1115–1118.
Pigati, J.S., Miller, D.M., Bright, J.E., Mahan, S.A., Nekola, J.C., Paces, J.B., 2011. Chronology, sedimentology, and microfauna of groundwater discharge deposits in the central Mojave Desert, Valley Wells, California. Geological Society of America Bulletin 123, 2224–2239.
Quade, J., 1986. Late Quaternary environmental changes in the upper Las Vegas Valley, Nevada. Quaternary Research 26, 340–357.
Quade, J., Mifflin, M.D., Pratt, W.L., McCoy, W., Burckle, L., 1995. Fossil spring deposits in the southern Great Basin and their implications for changes in water-table levels near Yucca Mountain, Nevada, during Quaternary time. Geological Society of America Bulletin 107, 213–230.
Ralph, F.M., Neiman, P.J., Wick, G.A., 2004. Satellite and CALJET aircraft observations of atmospheric rivers over the eastern North Pacific during the winter of 1997/98. Monthly Weather Review 132, 1721–1745.
Reheis, M.C., Miller, D.M., 2010. Environments of nearshore lacustrine deposition in the Pleistocene Lake Manix basin, south-central California. In: Reynolds, R.E., Miller, D.M. (Eds.), Overboard in the Mojave: 20 Million Years of Lakes and Wetlands: Abstracts of Proceedings, 2010 Desert Symposium, Zzyzx, Calif, pp. 24–37.
Reheis, M.C., Redwine, J.L., 2008. Lake Manix shorelines and Afton Canyon terraces: implications for incision of Afton Canyon. In: Reheis, M.C., Hershler, R., Miller, D.M. (Eds.), Late Cenozoic Drainage History of the Southwestern Great Basin and Lower Colorado River Region: Geologic and Biotic Perspectives. Geological Society of America Special Paper 439, Boulder, Colorado, pp. 227–260.
Reheis, M.C., Sarna-Wojcicki, A.M., Reynolds, R.L., Repenning, C.A., Mifflin, M.D., 2002. Pliocene to middle Pleistocene lakes in the western Great Basin: ages and connections. In: Hershler, R., Madsen, D.B., Currey, D.R. (Eds.), Great Basin Aquatic Systems History. Smithsonian Institution Press, Washington, D.C., pp. 53–108.
Reheis, M.C., Bright, J., Lund, S.P., Miller, D.M., Skipp, G., Fleck, R.J., 2012. A half-million-year record of paleoclimate from the Lake Manix core, Mojave Desert, California. Palaeogeography, Palaeoclimatology, Palaeoecology 365–366, 11–37.
Reheis, M.C., Adams, K.D., Oviatt, C.G., Bacon, S.N., 2014a. Pluvial lakes in the Great Basin of the western United States: a view from the outcrop. Quaternary Science Reviews 97, 33–57.
Reheis, M.C., Redwine, J.R., Wan, Elmira, McGeehin, J.P., Van Sistine, D.P., 2014b. Surficial geology and stratigraphy of Pleistocene Lake Manix, San Bernardino County, California. Scientific Investigations Map SIM-3312. U.S. Geological Survey.
Reimer, P.J., Baillie, M.G.L., Bard, E., Bayliss, A., Beck, J.W., Blackwell, P.G., Bronk Ramsey, C., Buck, C.E., Burr, G.S., Edwards, R.L., Friedrich, M., Grootes, P.M., Guilderson, T.P., Hajdas, I., Heaton, T.J., Hogg, A.G., Hughen, K.A., Kaiser, K.F., Kromer, B., McCormac, F.G., Manning, S.W., Reimer, R.W., Richards, D.A., Southon, J.R., Talamo, S., Turney, C.S.M., van der Plicht, J., Weyhenmeyer, C.E., 2009. IntCal09 and Marine09 radiocarbon age calibration curves, 0–50,000 years cal BP. Radiocarbon 51, 1111–1150.
Reimer, P.J., Bard, E., Bayliss, A., Beck, J.W., Blackwell, P.G., Ramsey, C.B., Buck, C.E., Cheng, H., Edwards, R.L., Friedrich, M., Grootes, P.M., Guilderson, T.P., Haflidason, H., Hajdas, I., Hatter, C., Heaton, T.J., Hoffmann, D.L., Hogg, A.G., Hughen, K.A., Kaiser, K.F., Kromer, B., Manning, S.W., Niu, M., Reimer, R.W., Richards, D.A., Scott, E.M., Southon, J.R., Staff, R.A., Turney, C.S.M., van der Plicht, J., 2013. INTCAL13 and MARINE13 radiocarbon age calibration curves, 0–50,000 years cal BP. Radiocarbon 55, 1869–1887.
Reynolds, R.E., Reynolds, R.L., 1994. The isolation of Harper Lake basin. In: Reynolds, R.E. (Ed.), Off Limits in the Mojave Desert. San Bernardino County Museum Redlands, pp. 34–37.
Robert, C., 2004. Late Quaternary variability of precipitation in southern California and climatic implications: clay mineral evidence from the Santa Barbara Basin, ODP Site 893. Quaternary Science Reviews 23, 1029–1040.
Roy, P.D., Quiroz-Jimenez, J.D., Perez-Cruz, L.L., Lozano-Garcia, S., Metcalfe, S.E., Lozano-Santacruz, R., Lopez-Balbiaux, N., Sanchez-Zavala, J.L., Romero, F.M., 2013. Late Quaternary paleohydrological conditions in the drylands of northern Mexico: a summer precipitation proxy record of the last 80 cal ka BP. Quaternary Science Reviews 78, 342–354.
Rutz, J.J., Steenburgh, W.J., 2012. Quantifying the role of atmospheric rivers in the interior western United States. Atmospheric Science Letters 13, 257–261.
Schulz, M., 2002. On the 1470-year pacing of Dansgaard–Oeschger warm events. Paleoceanography 17. http://dx.doi.org/10.1029/2000PA000571 (4–1 to 4–9).
Sionneau, T., Bout-Roumazeilles, V., Meunier, G., Kissel, C., Flower, B.P., Bory, A., Tribovillard, N., 2013. Atmospheric re-organization during Marine Isotope Stage 3 over the North American continent: sedimentological and mineralogical evidence from the Gulf of Mexico. Quaternary Science Reviews 81, 62–73.
Smith, G.I., 2009. Late Cenozoic geology and lacustrine history of Searles Valley, Inyo and San Bernardino Counties, California. U.S. Geological Survey Professional Paper 1727 (115 pp.).
Smith, G.I., Bischoff, J.L., Bradbury, J.P., 1997. Synthesis of the paleoclimatic record from Owens Lake core OL-92. In: Smith, G.I., Bischoff, J.L. (Eds.), An 800,000-year Paleoclimatic Record from Core OL-92, Owens Lake, Southeast California. Geological Society of America Special Paper 317, Boulder, Colorado, pp. 143–160.
Springer, K., Manker, C.R., Pigati, J.S., Mahan, S.A., 2013. Dynamic response of desert wetlands to abrupt climate change. Geological Society of America Abstracts with Programs 45 (7), 258.
Steinmetz, J.J., 1987. Ostracodes from the late Pleistocene Manix Formation, San Bernardino County, California. In: Reynolds, J. (Ed.), Quaternary History of the Mojave DesertSan Bernardino County Museum Association Quarterly, San Bernardino 34. 3–4, pp. 46–47.
Stuiver, M., Reimer, P.J., 1993. Extended ^{14}C data base and revised calib 3.0 ^{14}C age calibration program. Radiocarbon 35, 215–230.
Svensson, A., Anderson, K.K., Bigler, M., Clausen, H.B., Dahl-Jensen, D., Davies, S.M., Johnsen, S.J., Muscheler, R., Perrenin, F., Rasmussen, S.O., Rothlisberger, R., Seierstad, L., Steffensen, J.P., Vinther, B.M., 2006. The Greenland Ice Core Chronology 2005, 15–42 ka. Part 2: comparison to other records. Quaternary Science Reviews 25, 3258–3267.
Szabo, B.J., Kolesar, P.T., Riggs, A.C., Winograd, I.J., Ludwig, K.R., 1994. Paleoclimatic inferences from a 120,000-yr calcite record of water-table fluctuation in Browns Room of Devils Hole, Nevada. Quaternary Research 41, 59–69.
Thompson, R.S., Whitlock, C., Bartlein, P.J., Harrison, S.P., Spaulding, W.G., 1993. Climatic changes in the western United States since 18,000 yr B.P. In: Wright, H.E.J., Kutzbach, J.E., Webb, T.I.I.I., Ruddiman, W.F., Street-Perrott, F.A., Bartlein, P.J. (Eds.), Global Climates Since the Last Glacial Maximum. University of Minnesota Press, Minneapolis, pp. 468–513.
Vazquez, J.A., Lidzbarski, M.I., 2012. High-resolution tephrochronology of the Wilson Creek Formation (Mono Lake, California) and Laschamp event using ^{238}U–^{230}Th SIMS dating of accessory mineral rims. Earth and Planetary Science Letters 357–358, 54–67.
Wagner, J.D.M., Cole, J.E., Beck, J.W., Patchett, P.J., Henderson, G.M., Barnett, H.R., 2010. Moisture variability in the southwestern United States linked to abrupt glacial climate change. Nature Geoscience 3, 110–113.
Wells, S.G., Brown, W.J., Enzel, Y., Anderson, R.Y., McFadden, L.D., 2003. Late Quaternary geology and paleohydrology of pluvial Lake Mojave, southern California. In: Enzel, Y., Wells, S.G., Lancaster, N. (Eds.), Paleoenvironments and paleohydrology of the Mojave and southern Great Basin Deserts. Geological Society of America Special Paper 368, Boulder, Colo., pp. 79–114.
Winograd, I.J., Landwehr, J.M., Coplen, T.B., Sharp, W.D., Riggs, A.C., Ludwig, K.R., Kolesar, P.T., 2006. Devils Hole, Nevada, [delta]18O record extended to the mid-Holocene. Quaternary Research 66, 202–212.
Yamamoto, M., Yamamuro, M., Tanaka, Y., 2007. The California current system during the last 136,000 years: response of the North Pacific High to precessional forcing. Quaternary Science Reviews 26, 405–414.
Zhang, R., Delworth, T.L., 2007. Impact of the Atlantic Multidecadal Oscillation on North Pacific climate variability. Geophysical Research Letters 34, L23708.
Zic, M., Negrini, R.M., Wigand, P.E., 2002. Evidence of synchronous climate change across the Northern Hemisphere between the North Atlantic and the northwestern Great Basin, United States. Geology 30, 635–638.
Zimmerman, S.R.H., Hemming, S.R., Hemming, N.G., Tomascak, P.B., Pearl, C., 2011. High-resolution chemostratigraphic record of late Pleistocene lake-level variability, Mono Lake, California. Geological Society of America Bulletin 123, 2320–2334.
Zimmerman, S.R.H., Steponaitis, E., Hemming, S.R., Zermeño, P., 2012. Potential for accurate and precise radiocarbon ages in deglacial-age lacustrine carbonates. Quaternary Geochronology 13, 81–91.

https://doi.org/10.1016/j.yqres.2014.11.003 Published online by Cambridge University Press